

NON-PLANAR SILICON OXIDATION:
AN EXTENSION OF THE DEAL-GROVE MODEL

by

BRIAN D. LEMME

B.S., University of Nebraska-Lincoln, 2000

A REPORT

submitted in partial fulfillment of the requirements for the degree

MASTER OF SCIENCE

Department of Chemical Engineering
College of Engineering

KANSAS STATE UNIVERSITY
Manhattan, Kansas

2009

Approved by:

Major Professor
Dr. James H. Edgar

Abstract

Silicon oxidation has been the cornerstone of the semiconductor industry for many years, so understanding and being able to predict the oxidation process is paramount. The most popular model to date is the Deal-Grove model for the thermal oxidation of planar silicon surfaces. The Deal-Grove model owes its popularity to the overall simplicity in which it was derived and the accuracy in which it predicts the oxidation of planar silicon geometries. Due to this popularity and accuracy it is desirable to extend the Deal-Grove model beyond flat surfaces to other geometries such as cylinders and spheres. Extending the Deal-Grove model to these types of geometries would allow the prediction of the oxidation of silicon nano-wires and silicon nano-crystals. Being able to predict the oxidation is attractive due to the recent progress of integration of silicon nano-wires and silicon nano-crystals into microelectronic devices.

Prediction of the oxidation of silicon cylinders (nano-wires) and spheres (nano-crystals) by simply utilizing the established planar Deal-Grove model results in highly exaggerated oxide thicknesses compared with empirical data. This exaggeration for small silicon cylinders and spheres is due to the effects of the reduction in the available surface area for oxidation along with the stress induced due to the volumetric expansion and viscous flow of the oxide on non-planar surfaces. These stress effects retard the oxidation rate in non-planar silicon geometries with respect to flat surfaces. This reduction in the oxidation rate is caused by the normal compressive stress which is normal to the SiO_2/Si interface due to the volumetric expansion during oxidation. This compressive stress reduces the reaction rate constant at the SiO_2/Si interface and thus retards the overall oxidation rate for silicon cylinders and spheres with respect to planar silicon. The focus of this paper will be to contrast cylindrical and spherical versions of the Deal-Grove model to the well established planar version. Surface area and stress effects will also be explored as they help explain the reduction in the oxidation rate for non-planar silicon geometries.

Table of Contents

List of Figures	iv
List of Tables	v
Acknowledgements	vi
Dedication	vii
CHAPTER 1 - Introduction	1
Background	1
CHAPTER 2 - Silicon Oxidation Models	7
Oxidation of Planar Silicon: Deal-Grove Model	7
Oxidation of Cylindrical Silicon: Modified Deal-Grove Model	20
Oxidation of Spherical Silicon: Modified Deal-Grove Model	28
CHAPTER 3 - Stress Effects	36
CHAPTER 4 - Comparison of Models and Experimental Data	42
CHAPTER 5 - Conclusion	46
References	49

List of Figures

Figure 1.1: Structure of amorphous SiO ₂ ^[10]	2
Figure 1.2: Schematic of thickness of Si consumed during thermal oxidation ^[10]	2
Figure 1.3: Oxide thickness versus oxidation time for (100), (110), and (111) orientated silicon by wet oxidation ^[10]	3
Figure 1.4: Schematic of a silicon nano-wire field effect transistor; the scale bar is 5 nm ^[13]	6
Figure 2.1: Model for the oxidation of silicon ^[2]	7
Figure 2.2: Oxidation rates of silicon in dry oxygen at various oxidation temperatures	11
Figure 2.3: Wet oxidation rates of silicon at various oxidation temperatures	11
Figure 2.4: Limiting forms of Deal-Grove model ^[10]	13
Figure 2.5: The effect of partial pressure of the oxidant on the parabolic rate constant for wet and dry oxidation at 1000°C and 1200°C ^[1, 16]	14
Figure 2.6: Temperature effect on the parabolic rate constant, B	15
Figure 2.7: The diffusivity of dry oxygen and water in fused silica as a function of temperature	18
Figure 2.8: Temperature effect on the linear rate constant, B/A	19
Figure 2.9: Schematic of an oxidized convex silicon surface	23
Figure 2.10: Planar and cylindrical diffusion coefficient comparison vs. oxide thickness (dry oxidation)	25
Figure 2.11: Silicon cylinder oxide thickness vs. time (dry oxygen, 800°C, r = 0.1 μm)	26
Figure 2.12: Planar and spherical diffusion coefficient comparison vs. oxide thickness	32
Figure 2.13: Silicon sphere oxide thickness vs. time (dry oxygen, 800°C, r = 0.1 μm)	33
Figure 3.1: Viscous stresses during oxide growth on convex Si structures; P = hydrostatic pressure in the oxide layer creating the tensile stress ^[2]	37
Figure 3.2: Evolution of stress components as a function of oxidation time for both convex and concave silicon geometries ^[2]	37
Figure 4.1: Oxide growth of convex and concave cylindrical silicon including stress effects ^[2] ..	43
Figure 4.2: Oxide growth of spherical silicon including stress effects ^[5]	44
Figure 4.3: Oxide thickness as function of starting diameter for silicon nano-wires ^[23]	45

List of Tables

Table 1.2: Si nano-wire electrical properties compared to a planar Si device ^[13]	6
Table 2.1: Rate constants for the dry oxidation of silicon ^[1]	17
Table 2.2: Rate constants for the wet oxidation of silicon ^[1]	17
Table 2.3: k_{sh}/k_{s+h} for dry oxidation at various temperatures.....	17
Table 2.4: k_{sh}/k_{s+h} for wet oxidation at various temperatures	18
Table 2.5: Equilibrium concentration of dry oxygen in SiO ₂ at various temperatures.....	19
Table 2.6: Equilibrium concentration of water in SiO ₂ at various temperatures	20

Acknowledgements

Originally I set out to earn my Master Degree as a personal goal. Pursuing my Masters Degree proved to be a daunting endeavor due to the requirement of balancing both family and work with the requirements of obtaining an advanced degree. Nevertheless the journey has proved to be fulfilling, stimulating, challenging, and satisfying. With the completion of this report, I am closer to achieving my personal goal.

I would like to start by thanking everyone in Kansas State University's Department of Chemical Engineering and Division of Continuing Education. The professionalism and dedication exhibited by the staff in each of these departments made attending Kansas State University via distance learning a rewarding experience. I would like to specifically thank Dr. James Edgar for his support and guidance with the development of my program of study. Additionally, I would like to extend my gratitude to all of the employees in the Human Resources department at Intel Corporation who proctored my exams. Finally, I would like to thank graduate committee for their support.

I am extremely grateful for all of the support that my family, friends, and co-workers have afforded me during my studies. A special thanks goes to my wife for her support and understanding. I would also like to thank my Mother and Father. Without their support during my undergraduate studies none of this would have been possible.

Dedication

I would like to dedicate this work to my loving wife. Without her unending support and understanding my goal of completing my Master Degree would not have come to fruition. I love you Kate.

CHAPTER 1 - Introduction

The main focus of this report will be to present Deal-Grove^[1] inspired silicon oxidation models for silicon cylinders as described by Kao, et al.^[2] and Liu, et al.^[3], and silicon spheres as described by Okada et al.^[4], Coffin, et al.^[5], Liao, et al.^[6] and Chen, et al.^[7]. These cylindrical and spherical silicon oxidation models will be compared and contrasted to the well established Deal-Grove^[1] model for oxidation of planar silicon. It is desirable to predict the oxidation of silicon cylinders and spheres by using the Deal-Grove^[1] model for planar silicon oxidation due to the model's overall simplicity. Thus the feasibility for estimating the steady state oxidation rates of nano-scale silicon cylinders (i.e. nano-wires) and spheres (i.e. nano-crystals) using the planar Deal-Grove^[1] model will be investigated. Additional complexities that need to be considered for modeling the steady state oxidation of silicon cylinders and spheres will also be investigated and discussed.

Background

In integrated circuit (IC) device manufacturing, thermal oxidation is one of various ways of producing a layer of oxide on the surface of an underlying planar single crystal semiconductor material^[8]. In IC device manufacturing, single crystal silicon (Si) is widely popular primarily for the ease in which it forms an excellent thermal oxide. The oxide formed during thermal oxidation of silicon is silicon dioxide (SiO₂). Thermal oxidation of silicon is a relatively easy process since silicon is prone to forming a stable oxide at room temperature in an oxidizing atmosphere. Thermal oxidation, as its name implies, is a process that uses high temperatures (800°C to 1200°C) to grow oxide layers with enhanced rates in oxidizing environments. The high temperature used in the thermal oxidation of silicon accelerates the oxidation process allowing for thicker oxide layers to be produced. Thermally grown silicon dioxide has the fewest defects in both the bulk oxide and at the Si/SiO₂ interface. It has an amorphous structure (Figure 1.1) and it also has the desired properties of: 1) being an excellent electrical insulator (resistivity > 10²⁰ ohm-cm, band gap ~ 9eV), 2) having a high break down electric field (> 10 MV/cm), 3) forming a stable and reproducible Si/SiO₂ interface, and 4) growing conformal on

exposed silicon surfaces [1]. The properties of thermally grown silicon dioxide make it a desirable material for integration in IC circuits, such as the gate oxide.

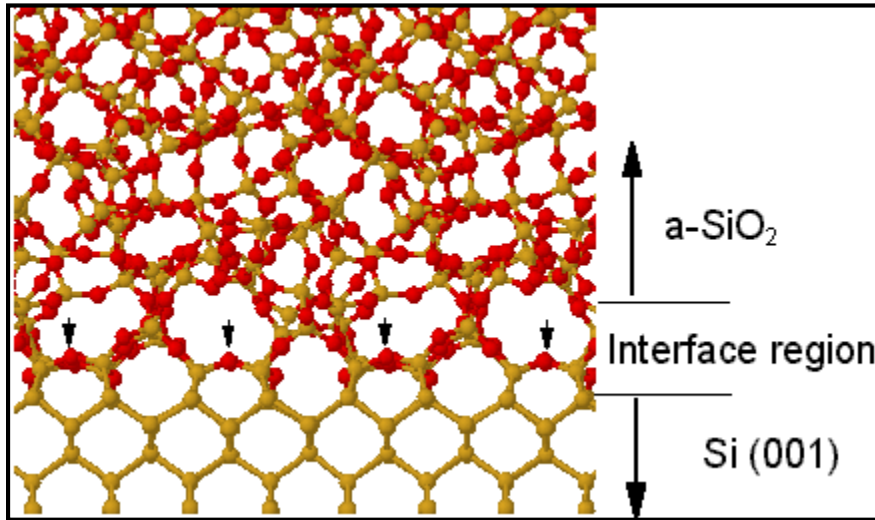


Figure 1.1: Structure of amorphous SiO_2 [10]

Other techniques for forming silicon dioxide include Chemical Vapor Deposition (CVD), Plasma Vapor Deposition (PVD), and High Density Plasma Deposition (HDP). These techniques deposit a layer of silicon dioxide on the semiconductor substrate, through a gas phase reaction, without consuming any of the underlying substrate material. In contrast the silicon substrate is consumed during thermal oxidation. For every 1 nano-meter (nm) of silicon consumed, 2.17 nm ($1 \text{ nm} = 10^{-9} \text{ m}$) of silicon oxide is created (Figure 1.2).

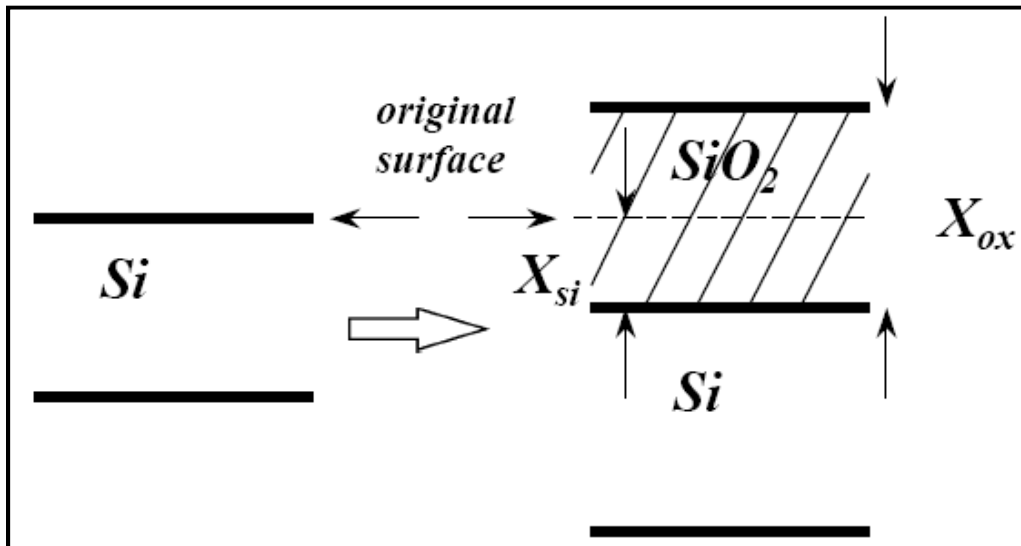


Figure 1.2: Schematic of thickness of Si consumed during thermal oxidation [10]

The oxidation rate of thermally grown silicon oxide is dependent on the surface density of Si-Si bonds, which depends on the crystal orientation of the silicon substrate. The silicon oxidation rate of silicon is fastest on the (111) orientation and is slowest on the (100) orientation, throughout the range of oxidation temperatures.^[11] For wet oxidation (111) and (100) crystallographic orientations bound the upper and lower oxidation rates for silicon, respectively (Figure 1.3).

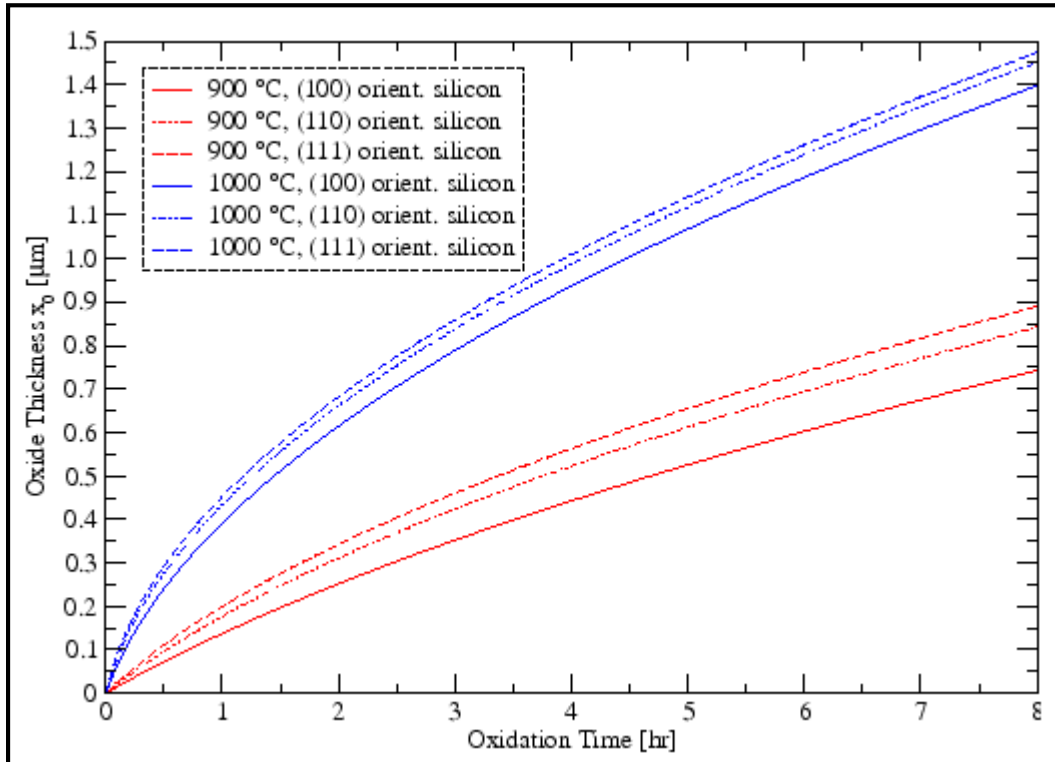
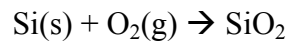
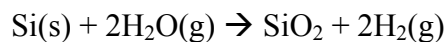


Figure 1.3: Oxide thickness versus oxidation time for (100), (110), and (111) orientated silicon by wet oxidation^[10]

There are two main processes for thermal oxidation of silicon, dry oxidation and wet oxidation. Dry oxidation uses molecular oxygen as that oxidant specie and proceeds according to the following overall reaction:



Wet oxidation of silicon uses water vapor instead of molecular oxygen as the oxidant species and proceeds according to the following overall reaction:



Both dry and wet thermal oxidation of silicon is typically carried out at temperatures ranging from 800°C to 1200°C, producing silicon oxide layers ranging in thickness from around 60 Angstroms to 10,000 Angstroms (1 Angstrom = 0.1 nm). The oxidation rate for both dry and wet oxidation increases dramatically with increased temperatures. Oxidant partial pressure also plays a critical role in the oxidation rate for both wet and dry oxidation. The oxidation rate increases nearly the same for both wet and dry oxidation as the partial pressure of the oxidant specie is increased. The wet oxidation of silicon has a higher overall growth compared to dry oxidation because the oxidant solubility limit in silicon dioxide is three orders of magnitude higher for water than oxygen ($3 \times 10^{19} \text{ cm}^{-3}$ for wet oxidation vs. $5.2 \times 10^{16} \text{ cm}^{-3}$ for dry oxidation at 1000°C). This fact makes wet oxidation preferable over dry oxidation of silicon for processes requiring the growth of thick silicon dioxide layers. However wet oxidation has a drawback; it produces a lower quality oxide compared to dry oxidation. Silicon oxide layers produced via wet oxidation have lower density, lower dielectric strength, and allow more current leakage at the Si/SiO₂ interface due to dangling Si bonds. The longer time required to grow silicon oxide layers by dry oxidation along with the higher quality silicon oxide produced typically limits this oxidation process to thin critical silicon oxide layers such as the gate oxide in MOSFET devices.

In the oxidation of silicon there are two main rate controlling regimes. After the initial regime where the thermal oxidation rate of the silicon is surface reaction rate controlled the oxidation of silicon transitions to a diffusion controlled process for both dry and wet oxidation. As the thickness of the silicon dioxide layer increases, the diffusion of molecular oxygen or water through the existing silicon dioxide layer increasingly dominates the oxidation rate of the silicon, which is proportional to the concentration of the oxidant specie at the Si/SiO₂ interface. The interface oxidant concentration is controlled by the diffusivity of molecular oxygen and water in silicon dioxide, which is much greater than the diffusivity of silicon in silicon dioxide. Thus, with thicker silicon dioxide layers, the growth rate is controlled by the diffusion of the oxidant specie(s) through the silicon dioxide layer. The diffusion in turn is controlled by the temperature and concentration of the oxidant in the bulk gas. Numerous mathematical models have been proposed to describe both dry and wet oxidation of planar silicon surfaces, such as silicon wafers used in semiconductor device manufacturing, taking into account the transport of the oxidant to the Si/SiO₂ interface.

The most popular mathematical model to date for describing both dry and wet oxidation of planar single crystal silicon surfaces was developed in 1965 by B. E. Deal and A. S. Grove^[1]. The model is affectionately known as the Deal-Grove^[1] model. The Deal-Grove^[1] model owes its popularity to its overall simplicity in describing the phenomena involved in planar silicon oxidation. The Deal-Grove^[1] model equates three fluxes involved in the oxidation of silicon: 1) transport of the oxidant (i.e. molecular oxygen or water vapor) from the bulk gas to the outer silicon dioxide surface, 2) transport of the oxidant across the SiO₂ film toward the silicon surface, and 3) reaction of the oxidant at the silicon surface forming a new layer of SiO₂. Equating these three fluxes and integrating the resulting differential equation results in the well known Deal-Grove^[1] equation for the thermal oxidation of planar silicon:

$$x_o^2 + Ax_o = B(t + \tau) \quad (1.1)$$

The quantity x_o is the total SiO₂ thickness, t is the oxidation time, τ is a quantity that corresponds to a shift in the time coordinate which corrects for the presence of the initial oxide layer, A is an equation coefficient and B is the parabolic rate constant.

As device dimensions have shrunk and device geometries have become more sophisticated, the oxidation of non-planar structures has become more common. The thermal oxidation of silicon is not limited to planar geometries, such as the oxidation of silicon wafers in planar semiconductor device manufacturing. Other geometries such as cylinders and spheres are also of interest due to ongoing research in nano-wire and nano-crystal technology. In particular, silicon nano-wires are attractive for their excellent physical and electrical properties (Table 1.1), and controllable diameters along with the prospect of integrating them into conventional IC technology using existing fabrication technology.^[12] The properties of silicon nano-wires depend strongly on the structure, shape and size, thus their control through techniques such as thermal oxidation is advantageous. These advantages make silicon nano-wires appealing as building blocks for the fabrication of next generation electronic and optoelectronic devices.

Recent progress has been reported for silicon nano-wire application in electronic devices (Figure 1.4) such as diodes, field-effect transistors (FETs), logic gates, single electron transistors, sensors, and solar cells^[7]. The development of nano-electronic devices makes the thermal oxidation of silicon nano-wires and nano-crystals important. First, thermally grown silicon dioxide forms an excellent interface to the silicon nano-wire substrate^[12]. Second, growing silicon dioxide on the surface of a silicon nano-wire by thermal oxidation is important for tuning

the final diameter of the silicon nano-wire. The underlying silicon nano-wire diameter can be controlled by thermally oxidizing the surface and then subsequently removing the oxide grown by chemical etching. Thus, the ability to predict the resulting thermal oxide thickness is important to properly control the silicon nano-wires to desired diameters, to attain the targeted electrical properties.

	nanowire data	planar Si device
gate length (nm)	50	50
gate oxide thickness (nm)	1.5	1.5
mobility ($\text{cm}^2/\text{V s}$)	230 - 1350	
I_{on} ($\mu\text{A}/\mu\text{m}$)	2000 - 5600	650
I_{off} ($\text{nA}/\mu\text{m}$)	4 - 45	9
subthreshold slope (mV/decade)	60	70
transconductance ($\mu\text{S}/\mu\text{m}$)	2700 - 7500	650

Table 1.1: Si nano-wire electrical properties compared to a planar Si device^[13]

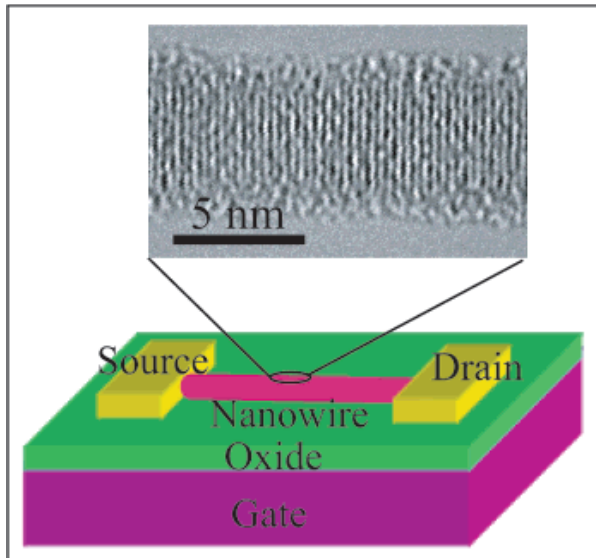


Figure 1.4: Schematic of a silicon nano-wire field effect transistor; the scale bar is 5 nm^[13]

CHAPTER 2 - Silicon Oxidation Models

Oxidation of Planar Silicon: Deal-Grove Model

B.E. Deal and A. S. Grove ^[1] presented their now popular model for thermal oxidation of planar silicon in 1965. Due to the simplicity of the model it is still applied frequently today in semiconductor device manufacturing. Deal and Grove derived their model by first considering a plane of silicon covered by a layer of silicon dioxide, x_0 thick (Figure 2.1). Two assumptions were made concerning the oxidation process:

1. the oxidation process is beyond an initial transient period, and
2. the oxidation proceeds by the inward movement of the oxidant species (i.e. oxygen and/or water) rather than by the outward movement of silicon.

Assumption number two is supported by experimental evidence for silicon ^[13, 14, 15] as reported by Deal and Grove ^[1]. The consequence of assumption number one is that the system is in steady state and thus three fluxes, F_1 through F_3 (Figure 2.1) are equal for all time.

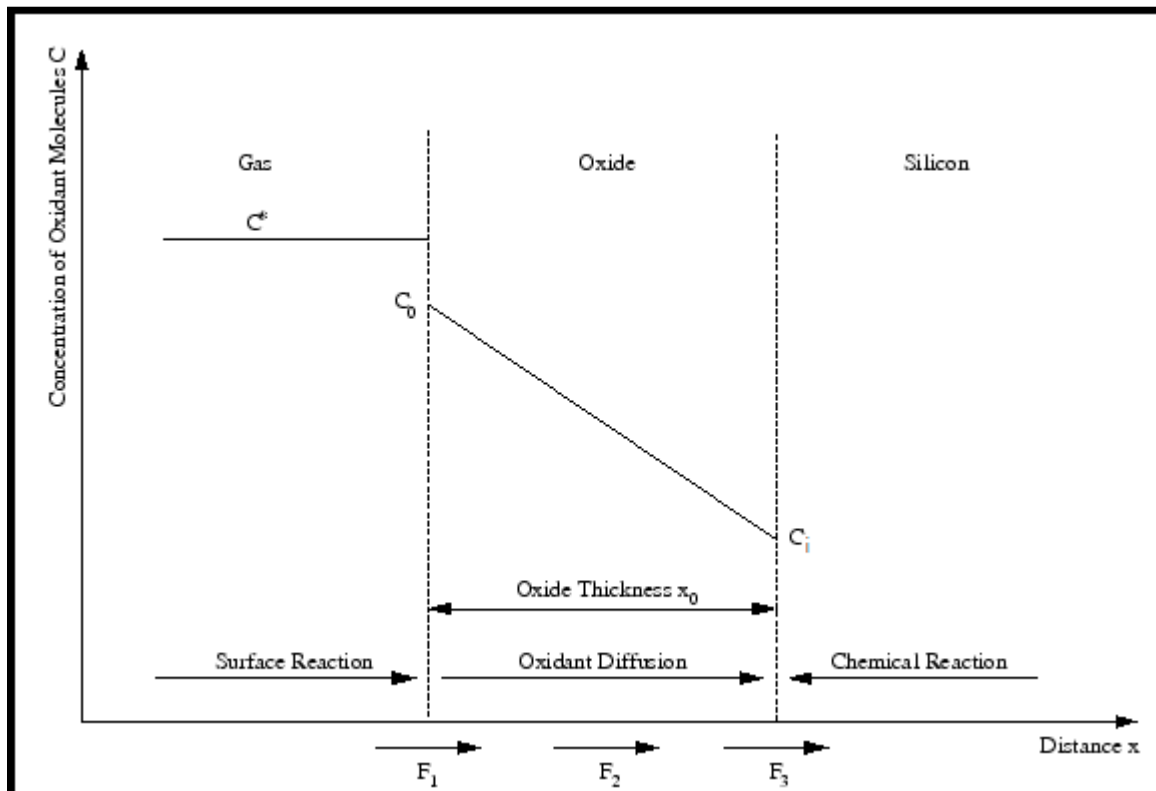


Figure 2.1: Model for the oxidation of silicon ^[2]

The oxidant specie(s) (i.e. oxygen and/or water) must go through the following steps, which represents the three fluxes (F_1 , F_2 and F_3), respectively ^[1]:

1. The oxidant (i.e. molecular oxygen or water vapor) is transported from the bulk gas to the outer silicon dioxide surface.
2. The oxidant is transported across the SiO_2 film toward the SiO_2/Si interface.
3. The oxidant reacts at the silicon surface forming a new layer of SiO_2 .

The flux of the oxidant from the bulk gas to the outer silicon dioxide surface (F_1) is represented as:

$$F_1 = h_G(C_G - C_S) \quad (2.1)$$

h_G = Mass transfer coefficient

C_G = Concentration of oxidant in the bulk gas

C_S = Concentration of the oxidant at the vicinity of the outer oxide surface

To determine the concentration of the oxidant at the outer surface of the oxide, C_o , Henry's law is employed to relate the outer surface oxidant concentration to the partial pressure of the oxidant in the bulk gas. Henry's law is only valid in the absence of oxidant association or dissociation at the outer surface of the oxide, which was shown empirically by Deal and Grove to be true.

$$C_o = HP_S \quad (2.2)$$

H = Henry's law constant for the oxidant in silicon dioxide

P_S = Partial pressure of the oxidant at the vicinity of the outer oxide surface

By using the ideal gas law:

$$C_S = \frac{N_S}{V} \quad (2.3)$$

$$P_S = \frac{N_S k T}{V} \quad (2.4)$$

k = Boltzmann's constant (1.3806×10^{-23} J/K)

T = Temperature of oxidant

V = Volume of oxidant gas

N_S = Number of oxidant molecules at the vicinity of the outer oxide surface

Thus:

$$C_o = HkTC_S = H\left(\frac{N_S k T}{V}\right) \quad (2.5)$$

$$C_s = \frac{C_o}{HkT} \quad (2.6)$$

Also, by defining the equilibrium concentration of the oxidant in the silicon dioxide layer (C^*) as:

$$C^* \equiv HkTC_G \quad (2.7)$$

Then the concentration of the oxidant in the bulk gas can be written as:

$$C_G = \frac{C^*}{HkT} \quad (2.8)$$

By utilizing equations 2.6 and 2.8 with equation 2.1 the flux of the oxidant from the bulk gas to the outer silicon dioxide surface is represented as:

$$F_1 = \frac{h_G}{HkT} (C^* - C_o) = h (C^* - C_o) \quad (2.9)$$

$$h \equiv \frac{h_G}{HkT} \quad (2.10)$$

The flux of the oxidant across the silicon dioxide film toward the silicon surface (F_2) is described by the one-dimensional form of Fick's first law of diffusion:

$$F_2 = -D \frac{\delta C}{\delta x} \quad (2.11)$$

D = Oxidant diffusivity in silicon dioxide

Assuming a linear concentration gradient of the oxidant in the silicon dioxide layer then equation 2.11 can be written as:

$$F_2 = D \frac{(C_o - C_i)}{x_o} \quad (2.12)$$

C_i = Oxidant concentration at the silicon/silicon dioxide interface

x_o = oxide thickness

The flux of the oxidant consumed by the reaction at the silicon/silicon dioxide interface (F_3) is given by:

$$F_3 = k_S C_i \quad (2.13)$$

k_S = Reaction rate constant at the silicon/silicon dioxide interface

The reaction rate constant, k_S , represents a number of chemical processes that take place at the silicon/silicon dioxide interface during oxidation. These include molecular oxygen dissociating to atomic oxygen, silicon to silicon bond breaking, and silicon and oxygen bond formation.

Due to the assumption that the oxidation process is beyond an initial transient period then due to this steady state condition:

$$F_1 = F_2 \text{ and } F_2 = F_3 \quad (2.14)$$

From the steady state assumption that yielded equation 2.14 the following two equations are obtained:

$$h(C^* - C_o) = D \frac{(C_o - C_i)}{x_o} \quad (2.15)$$

$$D \frac{(C_o - C_i)}{x_o} = k_S C_i \quad (2.16)$$

Equations 2.15 and 2.16 together create two equations with two unknowns, C_o and C_i . Solving equation 2.15 and 2.16 for C_o and C_i yields the following:

$$\frac{C_o}{C^*} = \frac{1 + \frac{k_S x_o}{D}}{1 + \frac{k_S}{h} + \frac{k_S x_o}{D}} \quad (2.17)$$

$$\frac{C_i}{C^*} = \frac{1}{1 + \frac{k_S}{h} + \frac{k_S x_o}{D}} \quad (2.18)$$

The oxidation rate is proportional to the flux of oxidant molecules to the silicon/silicon dioxide interface:

$$F = k_S C_i = \frac{k_S C^*}{1 + \frac{k_S}{h} + \frac{k_S x_o}{D}} \quad (2.19)$$

$$\frac{dx_o}{dt} = \frac{F}{N_1} = \frac{\frac{k_S C^*}{N_1}}{1 + \frac{k_S}{h} + \frac{k_S x_o}{D}} \quad (2.20)$$

N_1 = Number of oxidant molecules per unit volume required to form a unit volume of silicon dioxide ($2.25 \times 10^{22} \text{ cm}^{-3}$ for oxygen and $5 \times 10^{22} \text{ cm}^{-3}$ for water)

Equation 2.20 can be simplified by multiplying both the numerator and denominator by $2D/k_S$ resulting in:

$$\frac{dx_o}{dt} = \frac{B}{A + 2x_o} \quad (2.21)$$

$$A = 2D \left(\frac{1}{h} + \frac{1}{k_S} \right) \quad (2.22)$$

$$B = \frac{2DC^*}{N_1} \quad (2.23)$$

Equation 2.21 was employed to predict the oxidation rates for both dry and wet oxidation. The rate for wet oxidation is roughly 10 times faster than the dry oxidation rate. The results are graphed in Figures 2.2 and 2.3, respectively.

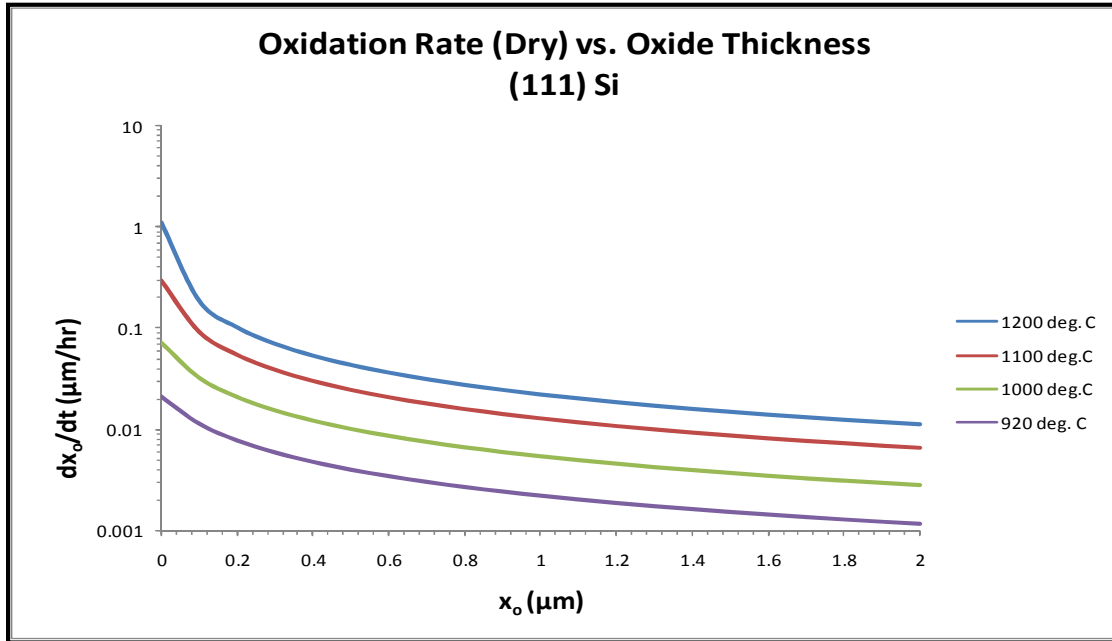


Figure 2.2: Oxidation rates of silicon in dry oxygen at various oxidation temperatures

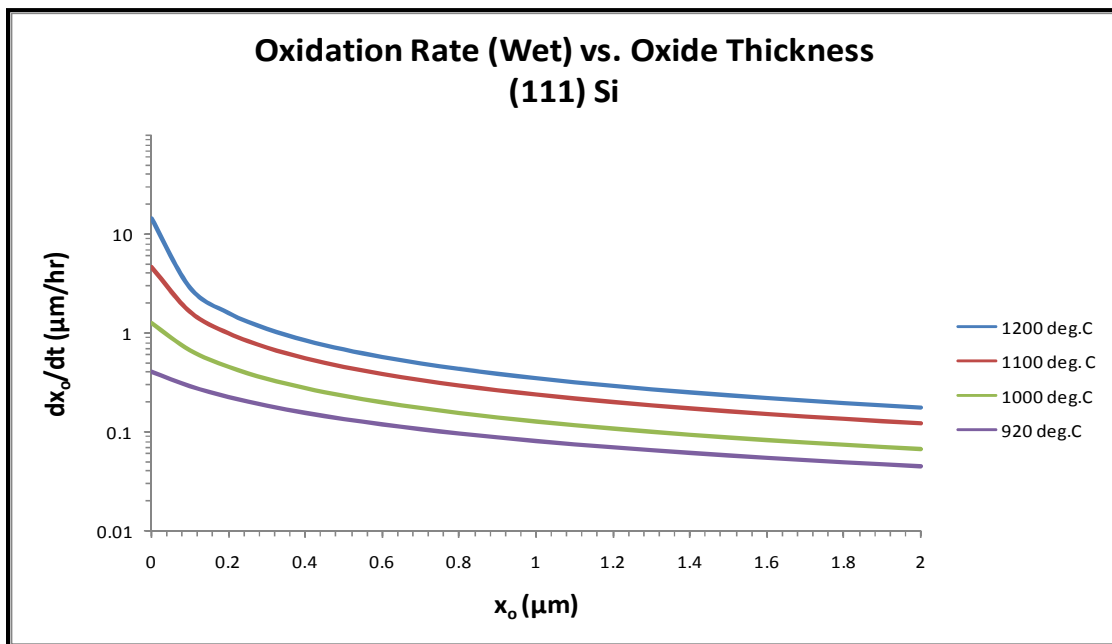


Figure 2.3: Wet oxidation rates of silicon at various oxidation temperatures

Deal and Grove^[1] arrived at initial conditions for equation 2.21 by considering a total oxide thickness, x_o , consisting of two parts; 1) an initial layer of oxide, x_i , and 2) the additional thickness of oxide grown during the thermal oxidation step. The initial layer of oxide, x_i is present on the silicon prior to the thermal oxidation under consideration. Thus Deal and Grove^[1] arrived at the following initial conditions for equation 2.21:

$$x_o = x_i \text{ at } t = 0 \quad (2.24)$$

The solution of equation 2.21 achieved through integration by separation of variables subject to the initial conditions from equation 2.24, is:

$$x_o^2 + Ax_o = x_i^2 + Ax_i + Bt \quad (2.25)$$

Equation 2.25 can be written in the more popular form:

$$x_o^2 + Ax_o = B(t + \tau) \quad (2.26)$$

where:

$$\tau = \frac{x_i^2 + Ax_i}{B} \quad (2.27)$$

To arrive at the oxide thickness as a function of time the quadratic equation 2.25 is solved yielding the following equation:

$$\frac{x_o}{A/2} = \left[1 + \frac{t + \tau}{A^2/4B}\right]^{1/2} - 1 \quad (2.28)$$

Deal and Grove^[1] examined two limiting forms of equation 2.28. The first limiting form was for large times (i.e. $t \gg A^2/4B$ and $t \gg \tau$), which yielded the following equation:

$$\frac{x_o}{A/2} = \left[\frac{t}{A^2/4B}\right]^{1/2} \text{ or } x_o^2 \cong Bt \quad (2.29)$$

The second limiting form was for the extreme of small oxidation times (i.e. $t \ll A^2/4B$), which yielded the following equation:

$$\frac{x_o}{A/2} = \frac{1}{2} \left(\frac{t + \tau}{A^2/4B}\right) \text{ or } x_o \cong \frac{B}{A}(t + \tau) \quad (2.30)$$

In equation 2.29 the coefficient B is referred to as the parabolic rate constant since equation 2.28 reduces to the well known parabolic oxidation law (Figure 2.4) for relatively long oxidation

times. The coefficient, $\frac{B}{A}$, in equation 2.30 is known as the linear rate constant since the general relationship given by equation 2.29 reduces to a linear law (Figure 2.4) for short oxidation times.

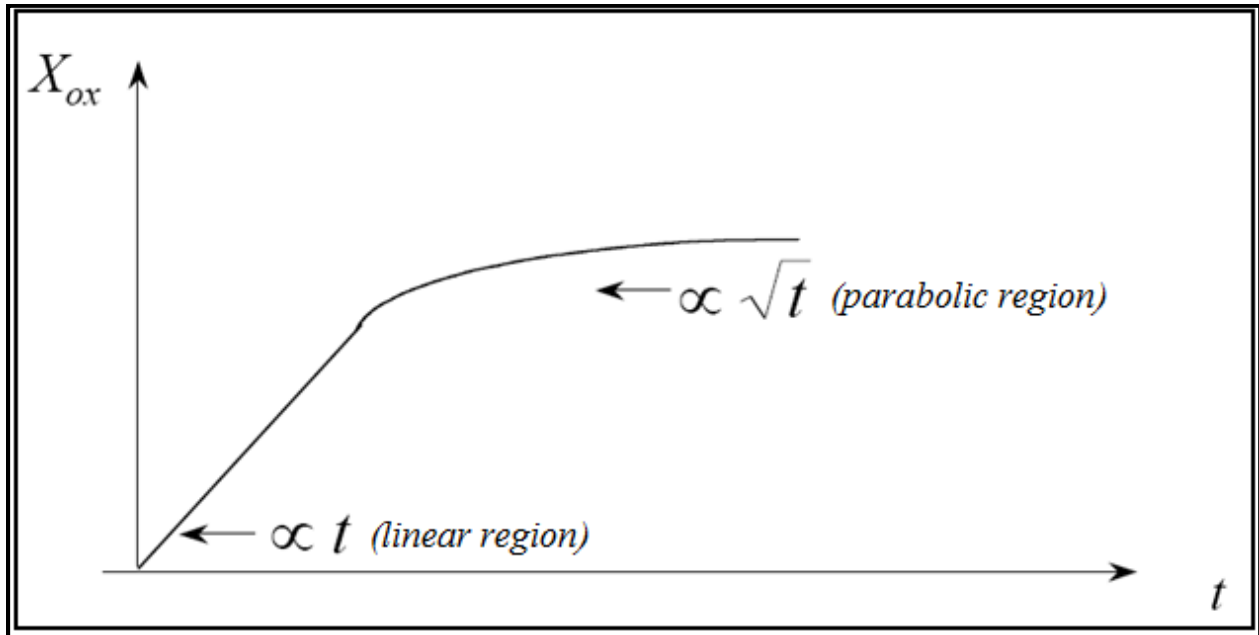


Figure 2.4: Limiting forms of Deal-Grove model ^[10]

According to equation 2.23 the parabolic rate constant, B , is proportional to the equilibrium oxidant concentration, C^* , in the oxide. If Henry's law is obeyed for the equilibrium oxidant concentration, C^* , then the parabolic rate constant, B , is also proportional to the partial pressure of the oxidizing species. This prediction has been experimentally verified (Figure 2.5). Also, according to equation 2.22 the coefficient A is independent on the partial pressure of the oxidizing species in the gas ^[17].

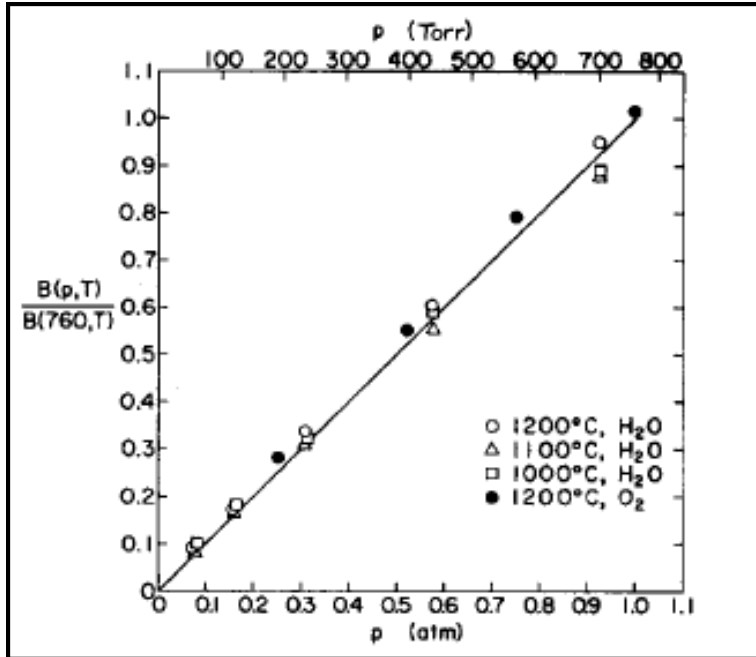


Figure 2.5: The effect of partial pressure of the oxidant on the parabolic rate constant for wet and dry oxidation at 1000°C and 1200°C [1, 16]

In the case of wet oxidation the initial oxide thickness, x_i , was found to be zero at all temperatures by extrapolating the oxide thickness to $t = 0$ on a plot of oxide thickness versus oxidation time. In contrast, a plot of oxide thickness versus oxidation time for dry oxygen oxidation extrapolated to $t = 0$ did not extrapolate to zero initial thickness at any temperature. This difference in extrapolated initial thickness for wet and dry oxidation explains the difference in the reported values for τ . Since dry oxidation does not extrapolate to zero thickness at $t = 0$, the quantity τ then adjusts the time coordinate for the presence of an initial thickness of oxide for dry oxidation, x_i (Table 2.1).

According to equation 2.23, the parabolic rate constant, B , is dependent on the diffusivity of the oxidant in silicon dioxide. In turn the temperature dependence of the parabolic rate constant should be equivalent to that of the diffusivity of the oxidant specie(s) in the oxide layer. The temperature dependence for the parabolic rate constant is shown in Figure 2.6.

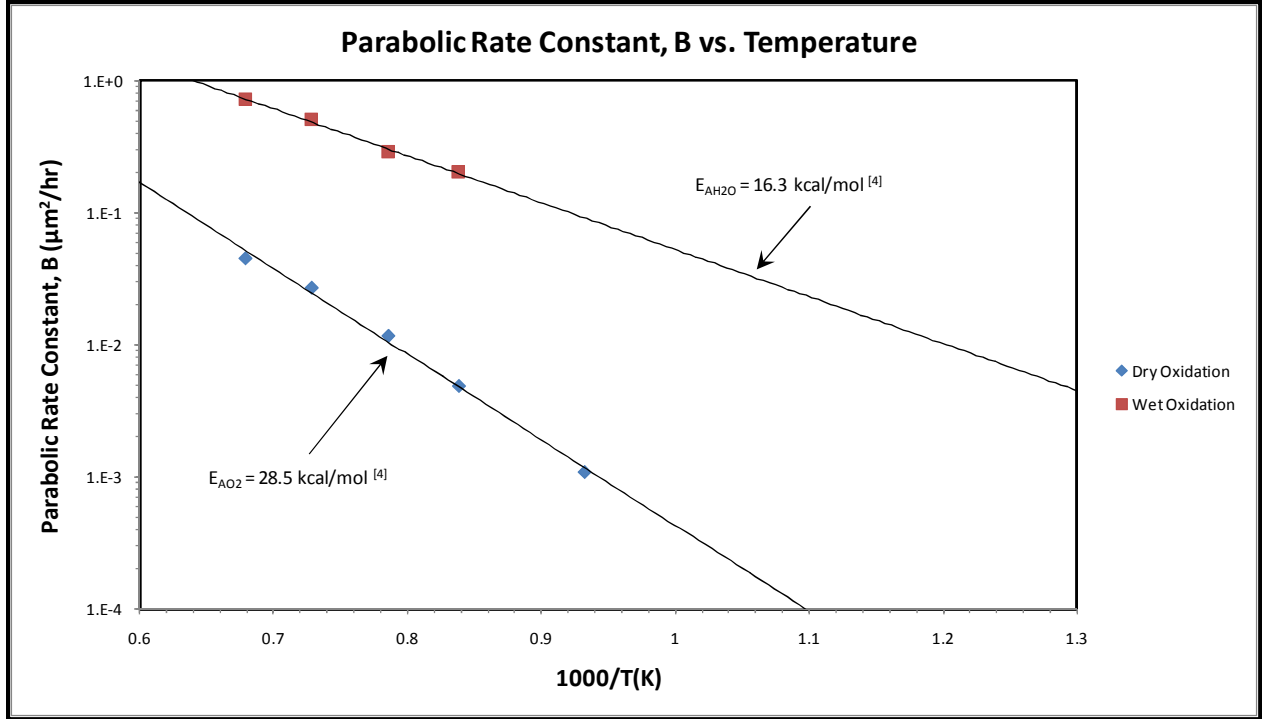


Figure 2.6: Temperature effect on the parabolic rate constant, B

The activation energies of B are 28.5 kcal/mol and 16.3 kcal/mol for dry oxygen and water, respectively [1]. The diffusivity of dry oxygen and water in fused silica (the structure of silicon dioxide formed through thermal oxidation corresponds to amorphous, fused silica) as a function of temperature is given in Figure 2.7. The diffusivity temperature dependence follows an Arrhenius functional relationship:

$$D_{O_2} = D_{O_2}^0 e^{-\frac{E_{O_2}}{RT}} \quad (2.31)$$

$$D_{H_2O} = D_{H_2O}^0 e^{-\frac{E_{H_2O}}{RT}} \quad (2.32)$$

where D_{O_2} and D_{H_2O} are the diffusivities of dry oxygen and water in silicon dioxide, respectively. The pre-exponential terms, $D_{O_2}^0$ and $D_{H_2O}^0$ have the values of $1.02 \times 10^8 \mu\text{m}^2/\text{hr}$ and $3.60 \times 10^5 \mu\text{m}^2/\text{hr}$ [18], respectively. The diffusivity activation energies are $E_{O_2} = 27 \text{ kcal/mol}$ [19] and $E_{H_2O} = 18.3 \text{ kcal/mol}$ [18] for dry oxygen and water, respectively. R is the universal gas constant and T is temperature. Thus, the diffusivity activation energies for dry oxygen and water are in good agreement with the activation energies of B for dry and wet oxidation.

Figure 2.8 shows the temperature dependence of the linear rate constant, B/A. It has an Arrhenius functional dependence with activation energies $E_{O_2} = 46 \text{ kcal/mol}^{[4]}$ and $E_{H_2O} = 45.3 \text{ kcal/mol}^{[1]}$ respectively for dry oxygen and water. A similar surface controlled mechanism is suggested for both dry oxygen and water since the activation energies for both of these oxidant species are essentially equal. The linear rate constant is given by dividing equation 2.23 by equation 2.22 yielding:

$$\frac{B}{A} = \frac{k_S h}{k_S + h} \left(\frac{C^*}{N_1} \right) \quad (2.33)$$

The linear rate constant, equation 2.33, includes the effects at both the gas/oxide interface (h) along with the oxide/silicon interface (k_S). If these quantities (h and k_S) are very different in magnitude, the quantity $\frac{k_S h}{k_S + h}$ will approximately equal k_S or h, whichever is smaller.^[4] Various calculated values for the quantity $\frac{k_S h}{k_S + h}$ are given in Table 2.3 and Table 2.4 for dry oxygen and water, respectively. Deal and Grove^[1] assumed that h is determined solely by a gas phase transport process where its value can be estimated based on standard boundary layer considerations. For the flows considered in the original work by Deal and Grove^[1] (Reynolds number ≈ 25) the value of h is estimated to be approximately $10^8 \text{ } \mu\text{m/hr}^{[1]}$. This relatively large value of the gas-phase transport coefficient, h was confirmed by Deal and Grove^[1] by two experiments. In the first experiment, the carrier gas flow rate was varied 50 fold without any significant effect on the oxidation rate. In the other experiment the backside of the silicon wafer, which was lying flat on the boat was oxidized to the same extent as the topside. Both of these observations by Deal and Grove^[1] point to the relatively small importance of the gas phase transport process in the overall oxidation process. Also, with most silicon oxidation being conducted at atmospheric pressure the oxidation rate is then approximately independent of the gas phase mass transport (h). With the value for h being several orders of magnitude large than the values for the quantity $\frac{k_S h}{k_S + h}$ given in Table 2.3 and Table 2.4 it follows that $\frac{k_S h}{k_S + h} = k_S$ since h is much larger than k_S . Thus, the activation energies for the linear rate constant, B/A for dry and wet oxidation reflect the temperature dependence of the reaction at the Si/SiO₂ interface. This temperature dependence of k_S is described using an Arrhenius function yielding the following equations for dry and wet oxidation:

$$k_{SO_2} = A_{O_2} e^{-\frac{E_{O_2}}{RT}} \quad (2.34)$$

$$k_{SH_2O} = A_{H_2O} e^{-\frac{E_{H_2O}}{RT}} \quad (2.35)$$

where the pre-exponential factors A_{O_2} and A_{H_2O} have average calculated values of 6.33×10^6 $\mu\text{m/hr}$ and 6.55×10^7 $\mu\text{m/hr}$, respectively. These values are based upon the linear rate constants, B/A given in Table 2.1 and Table 2.2 along with the activation energies for dry oxygen and water given in Figure 2.8.

Oxidation Temperature ($^{\circ}\text{C}$)	A (μm)	B ($\mu\text{m}^2/\text{hr}$)	B/A ($\mu\text{m}/\text{hr}$)	τ (hr)
1200	0.040	0.045	1.12	0.027
1100	0.090	0.027	0.30	0.076
1000	0.165	0.0117	0.071	0.37
920	0.235	0.0049	0.0208	1.40
800	0.370	0.0011	0.003	9.0
700			0.00026	81.0

Table 2.1: Rate constants for the dry oxidation of silicon ^[1]

Oxidation Temperature ($^{\circ}\text{C}$)	A (μm)	B ($\mu\text{m}^2/\text{hr}$)	B/A ($\mu\text{m}/\text{hr}$)	τ (hr)
1200	0.05	0.720	14.40	0
1100	0.11	0.510	1.64	0
1000	0.226	0.287	1.27	0
920	0.50	0.203	0.406	0

Table 2.2: Rate constants for the wet oxidation of silicon ^[1]

Oxidation Temperature ($^{\circ}\text{C}$)	$k_s h / k_s + h$ ($\mu\text{m}/\text{hr}$)
1200	5.0E+05
1100	1.1E+05
1000	2.8E+04
920	9.7E+03
800	1.7E+03

Table 2.3: $k_s h / k_s + h$ for dry oxidation at various temperatures

Oxidation Temperature ($^{\circ}\text{C}$)	$k_{\text{sh}}/k_{\text{s+h}}$ ($\mu\text{m/hr}$)
1200	$2.8\text{E}+04$
1100	$2.8\text{E}+03$
1000	$2.3\text{E}+03$
920	$6.4\text{E}+02$

Table 2.4: $k_{\text{sh}}/k_{\text{s+h}}$ for wet oxidation at various temperatures

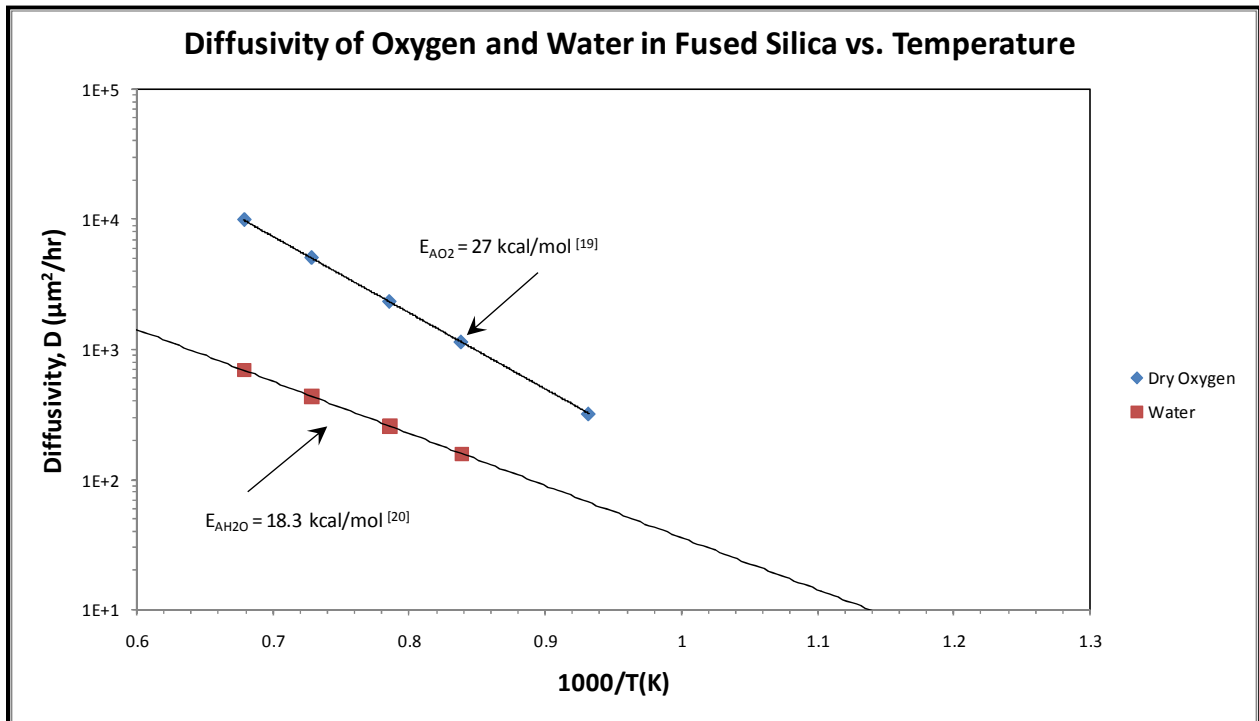


Figure 2.7: The diffusivity of dry oxygen and water in fused silica as a function of temperature

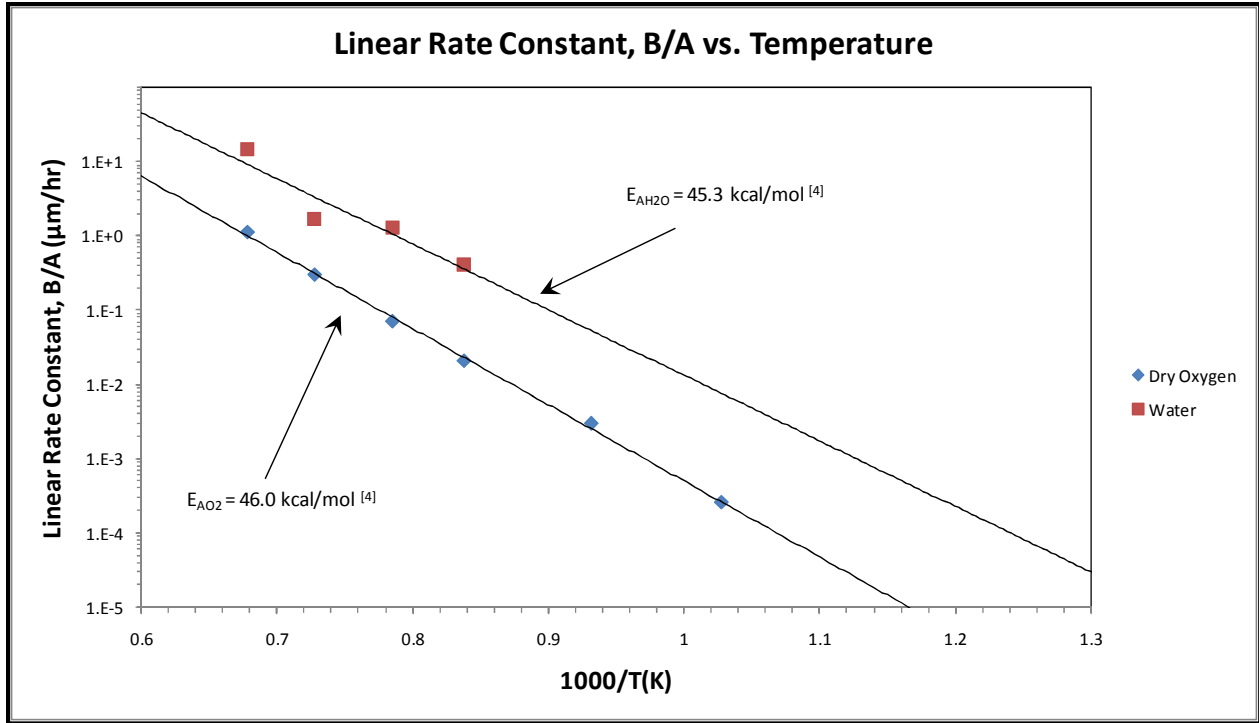


Figure 2.8: Temperature effect on the linear rate constant, B/A

The equilibrium concentration of the oxidants in silicon dioxide, C^* at various temperatures can be determined through exploiting equation 2.23 and either equation 2.31 or 2.32 depending on the oxidant specie of interest. Values for the parabolic rate constant, B can be either taken from Tables 2.1 and 2.2 or read from Figure 2.6. Values of C^* at various temperatures are given in Table 2.5 for dry oxygen and Table 2.6 for water.

Oxidation Temperature (°C)	C^* (cm^{-3})
1200	5.1E+16
1100	6.0E+16
1000	5.6E+16
920	4.8E+16
800	3.9E+16

Table 2.5: Equilibrium concentration of dry oxygen in SiO_2 at various temperatures

Oxidation Temperature (°C)	C* (cm ⁻³)
1200	2.6E+19
1100	2.9E+19
1000	2.8E+19
920	3.2E+19

Table 2.6: Equilibrium concentration of water in SiO₂ at various temperatures

As shown in both Table 2.5 and Table 2.6 the equilibrium concentrations for both dry oxygen and water in silicon dioxide are essentially constant with temperature due to the similarity in the temperature dependence of the parabolic rate constant, B and of the oxidant diffusivity.

The Deal-Grove^[1] model for thermal oxidation of planar silicon owes its popularity to its overall simplicity. Deal and Grove^[1] compared their model to experimental results and found it agreed well with the experimental data. The coefficients in the Deal-Grove^[1] model, namely A and B, were also shown to depend on pressure and temperature in a predictable manner^[1]. As shown above in equation 2.23 the parabolic rate constant, B, is proportional to the partial pressure of the oxidizing species. The coefficient, A, is independent of pressure as shown by equation 2.22. The parabolic rate constant, B, has an exponential temperature dependence due to the exponential temperature dependence of the diffusivities of oxygen and water in fused silica as shown by equation 2.23 and Figures 2.6 and 2.7. The equilibrium concentrations of both oxygen and water are essentially constant across the range of oxidation temperatures of interest as shown in Table 2.5 and Table 2.6. The values given in Table 2.5 and Table 2.6 for the equilibrium concentrations of oxygen and water are in good agreement with solubility of oxygen and water in silica.^[17, 18] Due to its simplicity, the planar Deal-Grove^[1] model has been modified to predict thermal oxidation rates of cylindrical and spherical silicon structures.

Oxidation of Cylindrical Silicon: Modified Deal-Grove Model

In the Deal-Grove^[1] model for thermal oxidation of planar silicon, the three fluxes (Figure 2.1) are set equal to each other (Equation 2.14). The planar Deal-Grove^[1] model is comparable to a steady state diffusion model for the oxidant (i.e. oxygen or water) which is described by the Laplace equation.^[2] An idealized modified Deal-Grove^[1] model for cylindrical silicon structures can be derived by extending the planar Deal-Grove^[1] model criteria and

assumptions into cylindrical coordinates. Also, to simplify the theoretical analysis the effect of crystal orientation on the rate of oxidation is assumed negligible as proposed by Kao et al. [2]

The diffusion of oxidizing species in cylindrical coordinates is described by the solution of the cylindrical version of the Laplace equation [2]:

$$\nabla^2 C = \frac{1}{r} \frac{\partial}{\partial r} \left(r \frac{\partial C}{\partial r} \right) = 0 \quad (2.36)$$

Again as in the Deal-Grove^[1] model for thermal oxidation of planar silicon the three fluxes (Figure 2.1) are set equal to each other. In cylindrical coordinates these fluxes are:

$$F_1 = h(C^* - C_o) \quad (2.37)$$

$$F_2 = D \frac{\partial C}{\partial r} \quad (2.38)$$

$$F_3 = k_s C_i \quad (2.39)$$

$$F_1 = F_2 \text{ and } F_2 = F_3 \quad (2.40)$$

$F_1 = F_2$ at the outer surface of the oxide layer (i.e. $r = b$) and $F_2 = F_3$ at the Si/SiO₂ interface (i.e. $r = a$) (Figure 2.9). Solving equation 2.36 by simple integration yields the following equation where k_1 and k_2 are constants of integration:

$$C(r) = k_1 \ln(r) + k_2 \quad (2.41)$$

Differentiating equation 2.41 with respect to r yields the following equation:

$$\frac{\partial C}{\partial r} = \frac{k_1}{r} \quad (2.42)$$

Evaluation of equation 2.42 at both interfaces (i.e. $r = a$ and $r = b$) produces the following two equations:

$$\frac{\partial C}{\partial r} \text{ at } r = a = \frac{k_1}{a} \quad (2.43)$$

$$\frac{\partial C}{\partial r} \text{ at } r = b = \frac{k_1}{b} \quad (2.44)$$

Combining equations 2.43 and 2.44 with equation 2.40 generates the following two equations:

$$h(C^* - C_o) = D \frac{k_1}{b} \quad (2.45)$$

$$D \frac{k_1}{a} = k_s C_i \quad (2.46)$$

Solving for C_o and C_i generates:

$$C_o = \frac{C^*hb - Dk_1}{hb} \quad (2.47)$$

$$C_i = \frac{Dk_1}{k_s a} \quad (2.48)$$

Noting that at $r = b$, $C = C_o$ and at $r = a$, $C = C_i$ and then evaluating equation 2.41 at $r = a$ and $r = b$ yields:

$$\frac{C^*hb - Dk_1}{hb} = k_1 \ln(b) + k_2 \quad (2.49)$$

$$\frac{Dk_1}{k_s a} = k_1 \ln(a) + k_2 \quad (2.50)$$

Equations 2.49 and 2.50 now contain two unknowns, k_1 and k_2 . Solving equations 2.49 and 2.50 for k_1 and k_2 produces:

$$k_1 = \frac{C^*}{\frac{D}{ak_s} + \frac{D}{bh} + \ln\left(\frac{b}{a}\right)} \quad (2.51)$$

$$k_2 = \frac{C^*(D - ak_s \ln(a))}{D + \frac{Dak_s}{bh} + ak_s \ln\left(\frac{b}{a}\right)} \quad (2.52)$$

Substituting equations 2.51 and 2.52 into equation 2.41 generates the following equation for the concentration of the oxidant as a function of the cylinder radius:

$$C(r) = \frac{C^*abhk_s}{Dbh + Dak_s + abhk_s \ln\left(\frac{b}{a}\right)} \left(\frac{D}{ak_s} + \ln\left(\frac{r}{a}\right) \right) \quad (2.53)$$

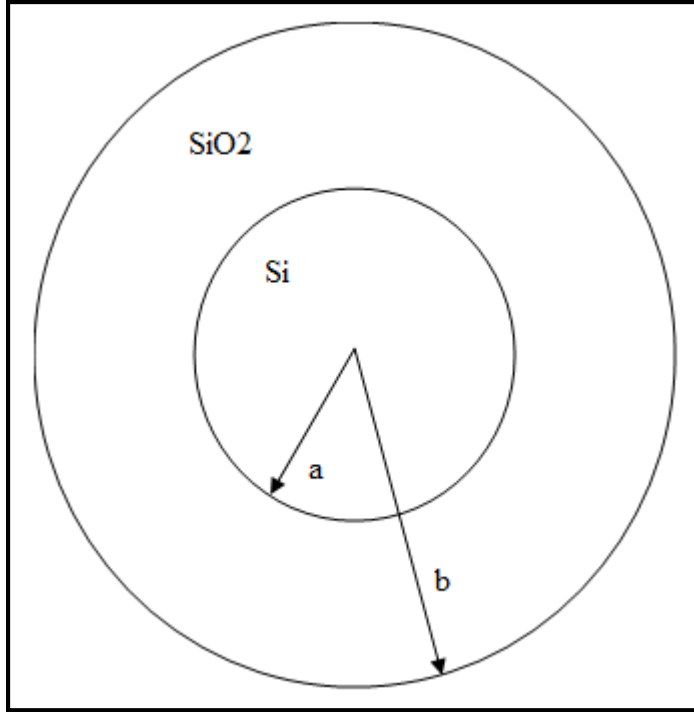


Figure 2.9: Schematic of an oxidized convex silicon surface

In order to develop an equation for the oxidation rate of a silicon cylinder one notes that the concentration of the oxidant molecules at the Si/SiO₂ interface is C_i at r = a. Thus solving equation 2.53 at r = a generates an expression for C_i:

$$C_i = \frac{C^*/k_s}{\frac{1}{k_s} + \frac{a}{b} \frac{1}{h} + \frac{a}{D} \ln\left(\frac{b}{a}\right)} \quad (2.54)$$

The oxidation rate is proportional to the flux of oxidant molecules to the Si/SiO₂ interface thus:

$$F = k_s C_i = \frac{C^*}{\frac{1}{k_s} + \frac{a}{b} \frac{1}{h} + \frac{a}{D} \ln\left(\frac{b}{a}\right)} \quad (2.55)$$

$$\frac{dx_o}{dt} = \frac{F}{N_1} = \frac{C^*/N_1}{\frac{1}{k_s} + \frac{a}{b} \frac{1}{h} + \frac{a}{D} \ln\left(\frac{b}{a}\right)} \quad (2.56)$$

It is also noted that the oxide thickness (x_o) for a silicon cylinder is given by:

$$x_o = b - a \text{ or } b = x_o + a \quad (2.57)$$

Thus equation 2.56 can be re-written in terms of the oxide thickness (x_o) by utilizing equation 2.57:

$$\frac{dx_o}{dt} = \frac{C^*/N_1}{\frac{1}{k_s} + \frac{a}{x_o} + \frac{1}{a} \frac{1}{h} + \frac{a}{D} \ln\left(1 + \frac{x_o}{a}\right)} \quad (2.58)$$

The diffusion of the oxidant species on a planar silicon surface is linearly dependent on the oxide thickness, x_o , as shown in equation 2.20 by the term x_o/D in the denominator. In contrast the diffusion of the oxidant species on a cylindrical silicon surface is logarithmically dependent on the oxide thickness, x_o , as shown in equation 2.58 by the term $\frac{a}{D} \ln\left(1 + \frac{x_o}{a}\right)$ in the denominator (Figure 2.10). Thus oxide thickness of silicon cylinders can no longer be predicted by means of the simple linear and parabolic rate constants as described by the Deal-Grove^[1] model for planar silicon oxidation. The logarithmic dependence of the diffusion coefficient in equation 2.58 is the main difference between equation 2.58 and the Deal-Grove^[1] Model, equation 2.20. The mass transfer terms ($1/h$) in the denominator of both equation 2.58 and 2.20 can be neglected because to it is the smallest term in the denominator of both equations. As the radius of silicon cylinders decrease, the coefficient for the diffusion term also decreases (Figure 2.10b). Thus for small diameter silicon cylinders with relatively thin oxide layers the reaction at the surface of the silicon dominates the oxidation rate as can be expect since the diffusion term in equation 2.58 approaches zero. As can be seen in Figure 2.10 for these conditions, either very small diameter silicon cylinders or relatively thin oxide layers, the diffusion coefficient in equation 2.58, $\frac{a}{D} \ln\left(1 + \frac{x_o}{a}\right)$, approaches zero and the oxidation process is increasingly dominated by the surface reaction rate. Thus for the case of thin oxides and/or small cylinder diameters the situation can be approximated by the use of the linear limiting form of planar Deal-Grove^[1] model. Although, as the oxide layer becomes thicker diffusion exhibits a more important role in the oxidation of silicon cylinders (Figure 2.10). As the silicon cylinder's oxide layer thickness increases the oxidation rate switches from reaction rate limited to diffusion limited similar to the oxidation of planar silicon. The planar Deal-Grove^[1] model can no longer adequately predict the oxidation rate as the oxide layer thickness increases on silicon cylinders.

In a cylindrical structure, a high concentration of oxidant is expected due to the wide exposure to the ambient^[2] as predicted by equation 2.53 with $r = a$. For a given oxide thickness the Si/SiO₂ interface concentration of oxidant, C_i , increases as the radius of the cylinder decreases. Also as can be seen in equation 2.58 when the oxide thickness, x_o , is thin relative to

the radius of the cylinder, a , equation 2.58 reduces to the Deal-Grove^[1] model for planar silicon oxidation, equation 2.20 (Figure 2.11).

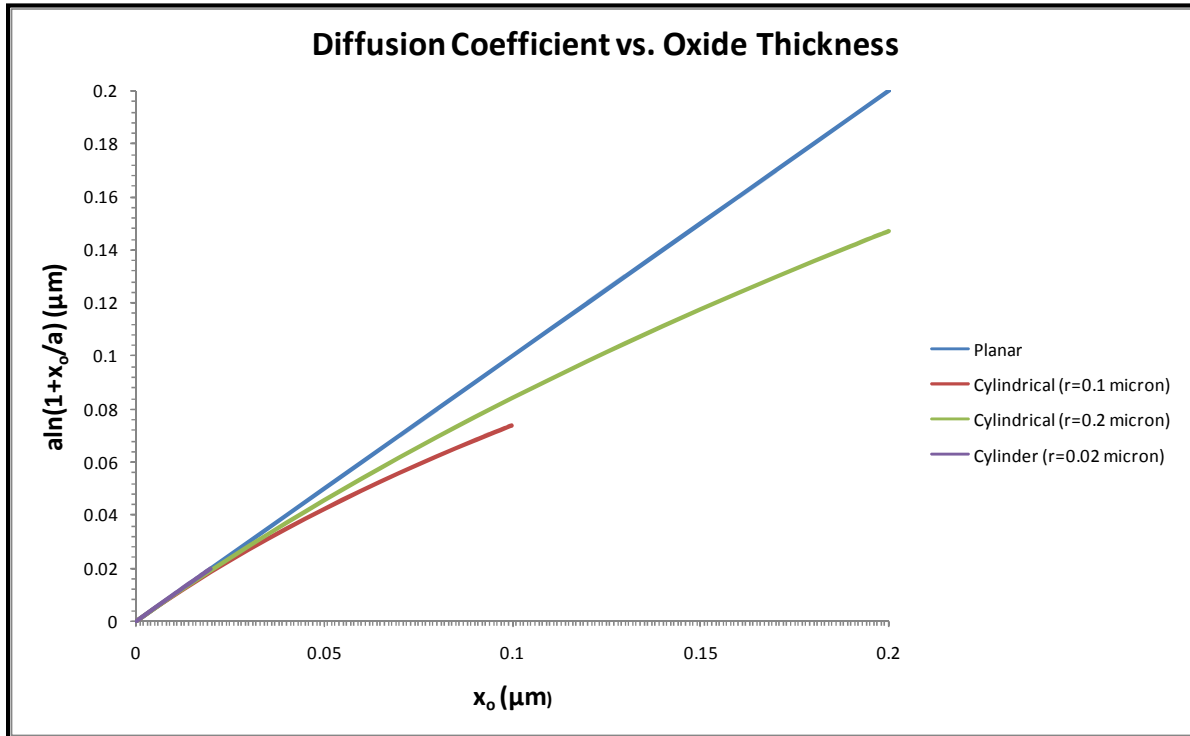


Figure 2.10: Planar and cylindrical diffusion coefficient comparison vs. oxide thickness (dry oxidation)

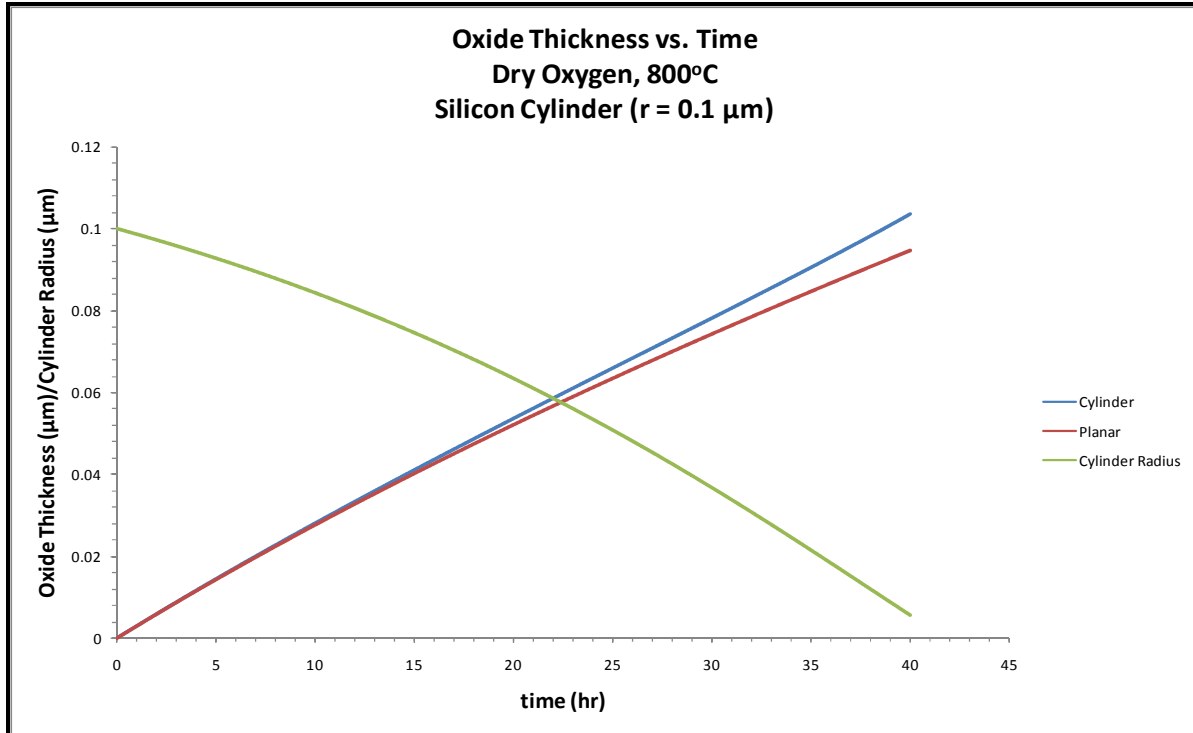


Figure 2.11: Silicon cylinder oxide thickness vs. time (dry oxygen, 800°C, r = 0.1 μm)

The oxidation of cylindrical silicon is also dependent on the surface area of the core silicon cylinder. The surface area during oxidation of planar silicon does not change with time. In contrast the surface area of a silicon cylinder does change with time and has to be taken into account when determining the oxide thickness at a given time. Due to the conservation of volume the core Si cylinder radius, $r = a$ (Figure 2.9), and the core Si cylinder radius + oxide shell radius, $r = b$ (Figure 2.9), are not independent variables.^[5,7] It is assumed that the oxide layer formed is an incompressible fluid.^[5,7] Also, it is assumed that the ratio of the volume of produced SiO₂ to the volume of consumed Si is 2.25:1 by the following relationship^[20]:

$$MW_{Si} = 28.086 \frac{gm}{mol} \text{ and } MW_{SiO_2} = 60.084 \frac{gm}{mol}$$

$$\rho_{Si} = 2.33 \frac{gm}{cm^3} \text{ and } \rho_{SiO_2} = 2.2 \frac{gm}{cm^3}$$

$$\frac{MW_{Si}}{\rho_{Si}} = 12.0541 \frac{cm^3}{mol} \text{ and } \frac{MW_{SiO_2}}{\rho_{SiO_2}} = 27.3109 \frac{cm^3}{mol}$$

$$\frac{MW_{SiO_2}/\rho_{SiO_2}}{MW_{Si}/\rho_{Si}} = \frac{27.3109 \text{ cm}^3/\text{mol}}{12.0541 \text{ cm}^3/\text{mol}} \cong 2.25 \quad (2.59)$$

where MW_{Si} and MW_{SiO_2} are the molecular weights of Si and SiO_2 , respectively and ρ_{Si} and ρ_{SiO_2} are the densities of Si and SiO_2 , respectively. The volume of a cylinder is:

$$V = \pi r^2 h \quad (2.60)$$

where r and h are the radius the height of the cylinder, respectively. If the starting radius of the core silicon cylinder is given by a_0 and the starting radius of the core silicon cylinder + oxide shell is given by b_0 , then a relationship between the core silicon cylinder, a , and the core silicon cylinder + oxide shell, b , can be developed through the following:

$$V_{SiO_2} = \pi(b^2 - a^2)h - \pi(b_0^2 - a_0^2)h \quad (2.61)$$

$$V_{Si} = \pi(a_0^2 - a^2)h \quad (2.62)$$

where V_{SiO_2} and V_{Si} are the volumes of the core silicon cylinder + oxide shell and the core silicon cylinder, respectively. Multiplying equation 2.62 by the value of 2.25 as given by equation 2.59 and then setting this equation equal to equation 2.61 yields the following equation:

$$\pi(b^2 - a^2)h - \pi(b_0^2 - a_0^2)h = 2.25\pi(a_0^2 - a^2)h \quad (2.63)$$

or

$$a^2 + 1.25b^2 = a_0^2 + 1.25b_0^2 = B$$

To develop a function describing how the core silicon cylinder radius, a , changes with time equation 2.63 is used along with the following equations:

$$V_{Si}(a) = \pi a^2 h \quad (2.64)$$

$$\frac{dV_{Si}}{dt} = 2\pi a h \frac{da}{dt} \quad (2.65)$$

$$V_{SiO_2}(a, b) = \pi(b^2 - a^2)h \quad (2.66)$$

$$\frac{dV_{SiO_2}}{dt} = 2\pi \left(b \frac{db}{dt} - a \frac{da}{dt} \right) h \quad (2.67)$$

$$\frac{dx_o}{dt} = \frac{db}{dt} - \frac{da}{dt} \quad (2.68)$$

Since one unit volume of Si is consumed and 2.25 unit volumes of SiO_2 are produced, the following relationship can be developed:

$$\frac{dV_{SiO_2}}{dt} = -2.25 \frac{dV_{Si}}{dt} \quad (2.69)$$

or

$$b \frac{db}{dt} - a \frac{da}{dt} = -2.25a \frac{da}{dt}$$

Solving equation 2.69 for da/dt yields the following differential:

$$\frac{da}{dt} = - \frac{dx_o}{dt} \frac{1}{1 + 1.25 \frac{a}{b}} \quad (2.70)$$

In order to eliminate b in equation 2.70 the relationship given by equation 2.63 is used resulting in the following differential equation describing how the core silicon cylinder radius, a, changes with time:

$$\frac{da}{dt} = - \frac{dx_o}{dt} \frac{1}{1 + 1.25a(B - 1.25a^2)^{-1/2}} \quad (2.71)$$

Combining equation 2.58 with equation 2.71 creates a system of two differential equations with two unknowns, x_o and a, which was solved numerically by means of a Runge-Kutta method (Figure 2.11).

In summary according to the model presented silicon cylinder will oxidizes faster than planar silicon for thick oxide layers (i.e. $\geq 0.5 \mu\text{m}$) and small diameters (Figure 2.11). Under the same conditions (thick oxide and small diameters), the oxidation rate for silicon cylinders is surface reaction rate controlled due to the small coefficient for the diffusion term in equation 2.58 (Figure 2.10) and also due to the higher interface concentration of oxidant, C_i . The oxidation rate of silicon cylinders come close to that of planar silicon, as describe by the Deal-Grove^[1] model, for relatively thin oxide layers and small cylinders, where the oxidation rate is reaction rate controlled, as described by equation 2.58. Thus in this situation the oxidation can be approximated with that of the planar Deal-Grove^[1] model.

Oxidation of Spherical Silicon: Modified Deal-Grove Model

In the Deal-Grove^[1] model for thermal oxidation of planar and cylindrical silicon, the three fluxes (Figure 2.1) are set equal to each other (Equation 2.14). The planar Deal-Grove^[1] model is comparable to a steady state diffusion model for the oxidant (i.e. oxygen or water) which is described by the Laplace equation.^[11,14] An idealized modified Deal-Grove^[1] model for spherical silicon structures can be derived by extending the Planar Deal-Grove^[1]

model criteria and assumptions into spherical coordinates as proposed by Coffin et al.^[5] and Chen et al.^[7] Also, as in the cylindrical oxidation model the effect of crystal orientation on the rate of oxidation is assumed negligible to simplify the theoretical analysis.

The diffusion of oxidizing species in spherical coordinates is described by the solution of the spherical version of the Laplace equation:

$$\nabla^2 C = \frac{1}{r^2} \frac{\partial}{\partial r} \left(r^2 \frac{\partial C}{\partial r} \right) = 0 \quad (2.72)$$

Again as in the Deal-Grove^[1] model for thermal oxidation of planar silicon the three fluxes (Figure 2.1) are set equal to each other. In spherical coordinates these fluxes are:

$$F_1 = h(C^* - C_o) \quad (2.73)$$

$$F_2 = D \frac{\partial C}{\partial r} \quad (2.74)$$

$$F_3 = k_s C_i \quad (2.75)$$

$$F_1 = F_2 \text{ and } F_2 = F_3 \quad (2.76)$$

$F_1 = F_2$ at the outer surface of the oxide layer (i.e. $r = b$) and $F_2 = F_3$ at the Si/SiO₂ interface (i.e. $r = a$) (Figure 2.9). Solving equation 2.72 by simple integration yields the following equation where k_1 and k_2 are constants of integration:

$$C(r) = \frac{k_1}{r} + k_2 \quad (2.77)$$

Differentiation equation 2.77 with respect to r yields the following equation:

$$\frac{\partial C}{\partial r} = \frac{-k_1}{r^2} \quad (2.78)$$

Evaluation of equation 2.78 at both interfaces (i.e. $r = a$ and $r = b$) produces the following two equations:

$$\frac{\partial C}{\partial r} \text{ at } r = a = \frac{-k_1}{a^2} \quad (2.79)$$

$$\frac{\partial C}{\partial r} \text{ at } r = b = \frac{-k_1}{b^2} \quad (2.80)$$

Combining equations 2.79 and 2.80 with equation 2.76 generates the following two equations:

$$h(C^* - C_o) = -D \frac{k_1}{b^2} \quad (2.81)$$

$$-D \frac{k_1}{a^2} = k_s C_i \quad (2.82)$$

Solving for C_o and C_i generates:

$$C_o = \frac{C^*b^2h + Dk_1}{b^2h} \quad (2.83)$$

$$C_i = \frac{-Dk_1}{a^2k_s} \quad (2.84)$$

Noting that at $r = b$, $C = C_o$ and at $r = a$, $C = C_i$ and then evaluating equation 2.77 at $r = a$ and $r = b$ yields:

$$\frac{-Dk_1}{a^2k_s} = \frac{k_1}{a} + k_2 \quad (2.85)$$

$$\frac{C^*b^2h + Dk_1}{b^2h} = \frac{k_1}{b} + k_2 \quad (2.86)$$

Equations 2.85 and 2.86 now contain two unknowns, k_1 and k_2 . Solving equations 2.85 and 2.86 for k_1 and k_2 produces:

$$k_1 = -\frac{C^*b^2h}{D\left(1 + \frac{hb^2}{k_s a^2}\right) + h\left(\frac{b^2}{a} - b\right)} \quad (2.87)$$

$$k_2 = -\frac{C^*\left(\frac{1}{k_s} + \frac{a}{D}\right)}{\frac{1}{k_s} + \frac{a^2}{b^2} \frac{1}{h} + \frac{1}{D}\left(a - \frac{a^2}{b}\right)} \quad (2.88)$$

Substituting equations 2.87 and 2.88 into equation 2.77 generates the following equation for the concentration of the oxidant as a function of the sphere radius:

$$C(r) = \frac{C^*(ra - a^2 + \frac{Dr}{k_s})}{r\left(\frac{Da^2}{b^2h} - \frac{a^2}{b} + a + \frac{D}{k_s}\right)} \quad (2.89)$$

In order to develop an equation for the oxidation rate of a silicon sphere one notes that the concentration of the oxidant molecules at the silicon/silicon dioxide interface is C_i at $r = a$. Thus solving equation 2.89 at $r = a$ generates an expression for C_i :

$$C_i = \frac{C^*/k_s}{\frac{1}{k_s} + \frac{a^2}{b^2} \frac{1}{h} + \frac{1}{D}\left(a - \frac{a^2}{b}\right)} \quad (2.90)$$

The oxidation rate is proportional to the flux of oxidant molecules to the Si/SiO₂ interface thus:

$$F = k_s C_i = \frac{C^*}{\frac{1}{k_s} + \frac{a^2}{b^2} \frac{1}{h} + \frac{1}{D}\left(a - \frac{a^2}{b}\right)} \quad (2.91)$$

$$\frac{dx_o}{dt} = \frac{F}{N_1} = \frac{C^*/N_1}{\frac{1}{k_s} + \frac{a^2}{b^2} \frac{1}{h} + \frac{1}{D} \left(a - \frac{a^2}{b}\right)} = \frac{C^*/N_1}{\frac{1}{k_s} + \frac{a^2}{b^2} \frac{1}{h} + \frac{a(b-a)}{bD}} \quad (2.92)$$

It is also noted that the oxide thickness (x_o) for a silicon sphere is given by:

$$x_o = b - a \text{ or } b = x_o + a \quad (2.93)$$

Thus equation 2.92 can be re-written in terms of the oxide thickness (x_o) by utilizing equation 2.93:

$$\frac{dx_o}{dt} = \frac{C^*/N_1}{\frac{1}{k_s} + \frac{a^2}{(x_o + a)^2} \frac{1}{h} + \frac{ax_o}{(x_o + a)} \frac{1}{D}} \quad (2.94)$$

The diffusion of the oxidant species on a planar silicon surface is linearly dependent on the oxide thickness, x_o , as shown in equation 2.20 by the term x_o/D in the denominator. In contrast the diffusion of the oxidant species on a spherical silicon surface is dependent on the ratio of the product of core silicon sphere radius, a , and the oxide thickness, x_o , to the core silicon sphere radius + oxide shell thickness, b or $x_o + a$, as shown in denominator of equation 2.94 by the term $\frac{ax_o}{(x_o+a)}$ (Figure 2.11). The dependence of the diffusion coefficient in equation 2.94 on the ratio of $\frac{ax_o}{(x_o+a)}$ is essentially the only difference between equation 2.94 and the Deal-Grove^[1] model, equation 2.20. As in the planar and cylindrical geometry cases, the mass transfer terms ($1/h$) in the denominator of both equation 2.94 and 2.20 can be neglected because it is the smallest term in the denominator of both equations. As the radius of silicon spheres decrease the coefficient for the diffusion term decreases (Figure 2.12). So for extremely thin oxides relative to the sphere radius the diffusion coefficient in equation 2.94 approaches zero. In this limiting form the oxidation process of silicon spheres is surface reaction rate limited and thus can be predicted using the linear limiting form of the planar Deal-Grove^[1] model (Figure 2.12). However, as the oxide thickness increases the diffusion term dominates in equation 2.94 and thus the oxidation process of silicon spheres can no longer be adequately predicted by the planar Deal-Grove^[1] model.

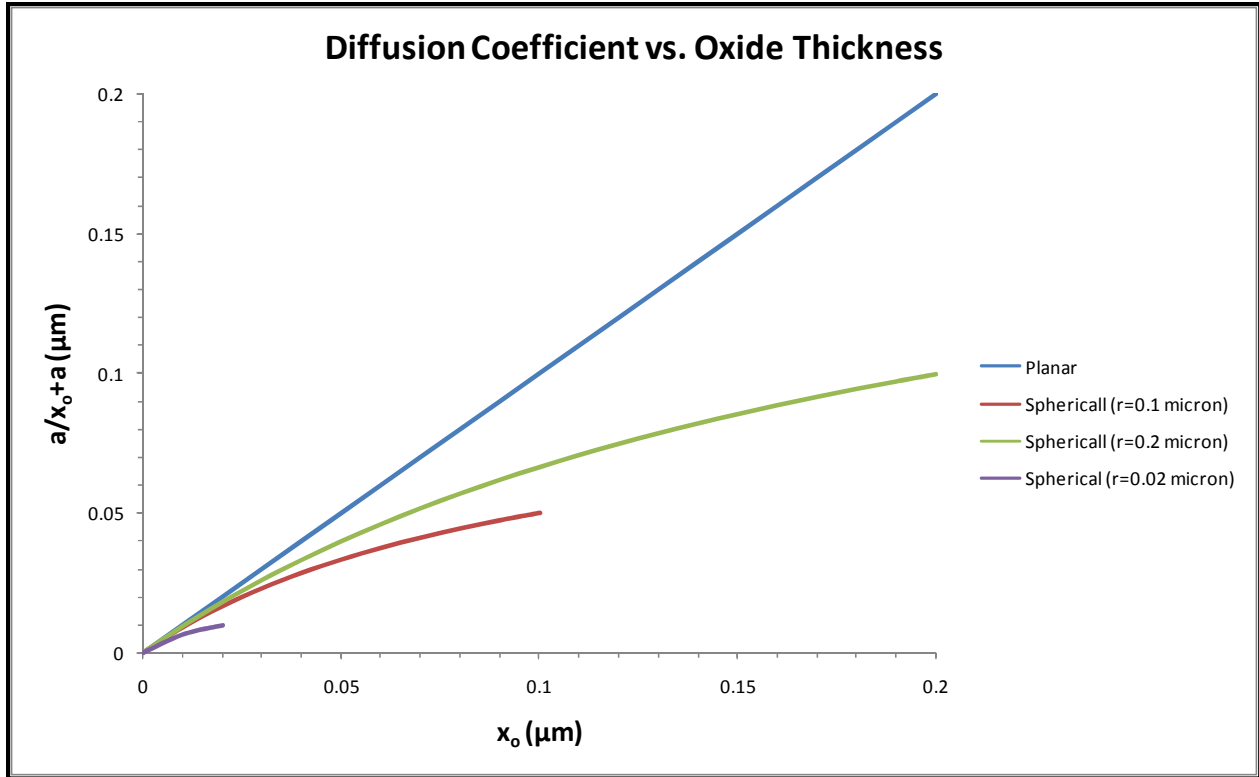


Figure 2.12: Planar and spherical diffusion coefficient comparison vs. oxide thickness

In a spherical structure, a high concentration of oxidant is expected due to the wide exposure to the ambient ^[2]. For a given oxide thickness the Si/SiO₂ interface concentration of oxidant, C_i , increases as the radius of the sphere decreases as described by equation 2.89 with $r = a$. Also as can be seen in equation 2.94 when the oxide thickness, x_o , is thin relative to the radius of the sphere, a , equation 2.94 reduces to the Deal-Grove^[1] model for planar silicon oxidation, equation 2.20 (Figure 2.13). Thus for the case of thin oxides and large spheres the situation can be approximated by the use of the planar Deal-Grove^[1] model.

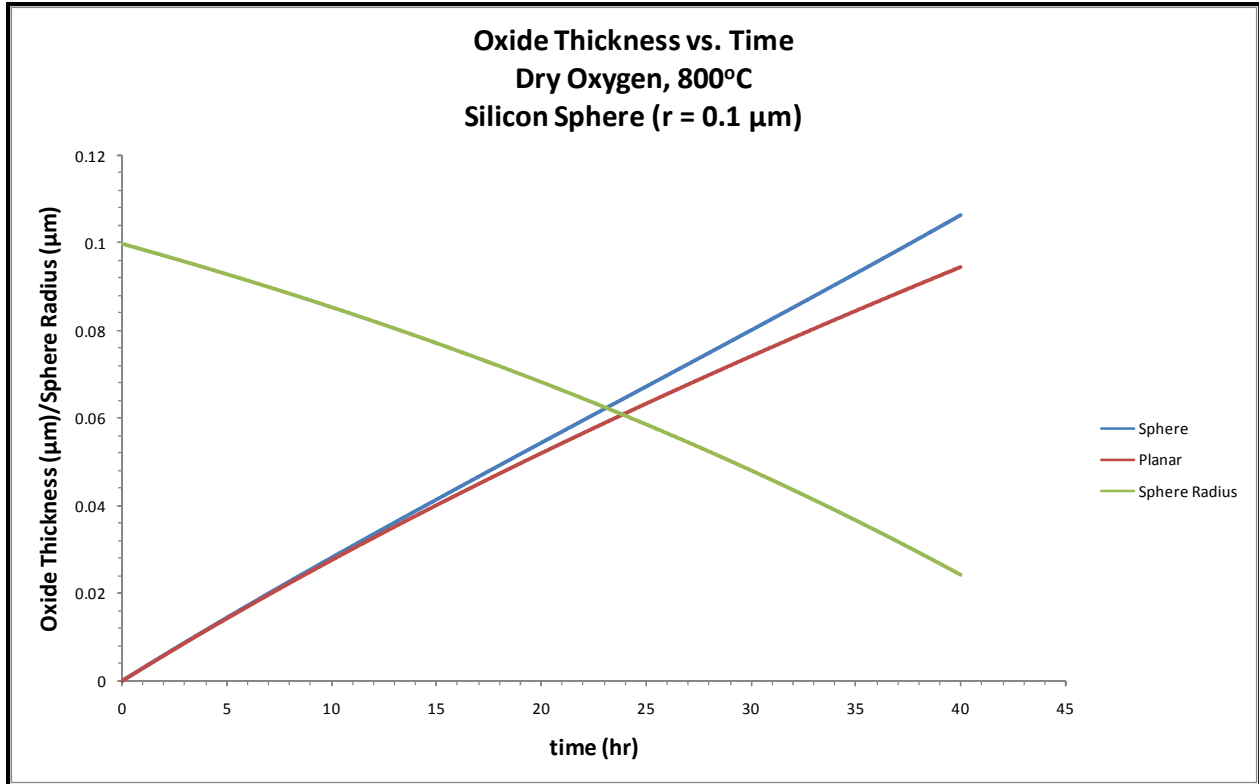


Figure 2.13: Silicon sphere oxide thickness vs. time (dry oxygen, 800oC, r =0.1μm)

As in the oxidation of cylindrical silicon, spherical silicon is also dependent on the surface area of the core silicon sphere. Also, as with cylindrical silicon the surface area of a silicon sphere does change with time and has to be taken into account when determining the oxide thickness at a given time. This is again in contrast to the oxidation of planar silicon where the surface area does not change with time. As was with cylindrical silicon, the conservation of volume the core Si sphere radius, $r = a$ (Figure 2.9), and the core Si sphere radius + oxide shell radius, $r = b$ (Figure 2.9), are not independent variables.^[5, 7] The same assumptions used for cylindrical silicon apply to spherical silicon. Namely, it is assumed that the oxide layer formed is an incompressible fluid^[5, 7]. Also, it is assumed that the ratio of the volume of produced SiO_2 to the volume of consumed Si is 2.25:1 by following the relationship in equation 2.59^[20]:

The volume of a sphere is:

$$V = \frac{4}{3}\pi r^3 \quad (2.95)$$

where r is the radius of the sphere. If the starting radius of the core silicon cylinder is given by a_0 and the starting radius of the core silicon sphere + oxide shell is given by b_0 then a relationship

between the core silicon sphere, a, and the core silicon sphere + oxide shell, b, can be developed through the following:

$$V_{SiO_2} = \frac{4}{3}\pi(b^3 - a^3) - \frac{4}{3}\pi(b_o^3 - a_o^3) \quad (2.95)$$

$$V_{Si} = \frac{4}{3}\pi(a_o^3 - a^3) \quad (2.96)$$

where V_{SiO_2} and V_{Si} are the volumes of the core silicon sphere + oxide shell and the core silicon sphere, respectively. Equating equation 2.96 with equation 2.97 and utilizing the relationship given by equation 2.59 yields the following equation:

$$\frac{4}{3}\pi(b^3 - a^3) - \frac{4}{3}\pi(b_o^3 - a_o^3) = 2.25 \frac{4}{3}\pi(a_o^3 - a^3) \quad (2.97)$$

or

$$a^3 + 1.25b^3 = a_o^3 + 1.25b_o^3 = B$$

To develop a function describing how the core silicon sphere radius, a, changes with time equation 2.97 is used along with the following equations:

$$V_{Si}(a) = \frac{4}{3}\pi a^3 \quad (2.98)$$

$$\frac{dV_{Si}}{dt} = 4\pi a^2 \frac{da}{dt} \quad (2.99)$$

$$V_{SiO_2}(a, b) = \frac{4}{3}\pi(b^3 - a^3) \quad (2.100)$$

$$\frac{dV_{SiO_2}}{dt} = 4\pi(b^2 \frac{db}{dt} - a^2 \frac{da}{dt}) \quad (2.101)$$

$$\frac{dx_o}{dt} = \frac{db}{dt} - \frac{da}{dt} \quad (2.102)$$

Now utilizing the fact that as one unit volume of Si is consumed 2.25 unit volumes of SiO_2 are produced the following relationship is developed:

$$\frac{dV_{SiO_2}}{dt} = -2.25 \frac{dV_{Si}}{dt} \quad (2.103)$$

or

$$b^2 \frac{db}{dt} - a^2 \frac{da}{dt} = -2.25 a^2 \frac{da}{dt}$$

Solving equation 2.103 for da/dt yields the following differential:

$$\frac{da}{dt} = -\frac{dx_o}{dt} \frac{1}{1 + 1.25 \frac{a^2}{b^2}} \quad (2.104)$$

In order to eliminate b in equation 2.104 the relationship given by equation 2.97 is used resulting in the following differential equation describing how the core silicon cylinder radius, a, changes with time:

$$\frac{da}{dt} = -\frac{dx_o}{dt} \frac{1}{1 + 1.25a^2(B - 1.25a^3)^{-2/3}} \quad (2.105)$$

Combining equation 2.94 with equation 2.105 creates a system of two differential equations with two unknowns, x_o and a, which was solved numerically by means of a Runge-Kutta method (Figure 2.13).

In summary according to the model presented a silicon sphere will oxidizes faster than planar silicon for thick oxide layers (i.e. $\geq 0.5 \mu\text{m}$) and small diameters. Under the same conditions (thin oxide and/or small diameters) the oxidation rate for silicon spheres is surface reaction rate controlled due to the small coefficient for the diffusion term in equation 2.94 and also due to the higher interface concentration of oxidant, C_i . The oxidation rate of silicon spheres come close to that of planar silicon, as describe by the Deal-Grove^[1] model, for relatively thin oxide layers.

CHAPTER 3 - Stress Effects

The two modified Deal-Grove^[1] models for the oxidation of silicon cylinders and silicon spheres presented in chapter 2 are simple models in that neither one accounts for the retarded oxidation caused by stress at the Si/SiO₂ interface and in the bulk oxide (Figure 3.1 and Figure 3.2) as the oxide layer increases in thickness. Kao et al.^[2] propose that the stress at the Si/SiO₂ interface and in the bulk oxide effect the reaction rate and transport of oxidants, respectively. It is assumed that SiO₂ is a viscous fluid and, in fact this assumption is reported to be valid above the viscous flow point (950°C), while at low temperatures (below 800°C) SiO₂ behaves as an elastic solid.^[5] It is expected above the elastic point (800°C) and below the viscous flow point (950°C) the oxidation of non-planar Si structures is retarded due to the normal stress induced at the Si/SiO₂ interface.^[5] The stress at the Si/SiO₂ interface is a result of expansion in volume as the reaction at the Si/SiO₂ interface proceeds. The volume of SiO₂ is larger than the initial volume of Si and as a result the material expands.^[9,11] The newly formed oxide pushes the old oxide, which rearranges itself through viscous flow.^[9,11] As the newly formed oxide presses on the old oxide the new oxide faces a resistance from the normal stress perpendicular to the surface.^[2] This normal stress hinders oxidation and thus the oxidation is retarded with respect to planar oxidation.^[2] Stress is also generated in the old bulk oxide by non-uniform deformation; the old oxide is under tension as it is being pushed out by the newly formed oxide layer creating a tensile stress. The old bulk oxide experiences non-uniform deformation due to the different rates of oxidation on the surface of a silicon cylinder and sphere. The dissimilar rates of oxidation on the surface is due to the different silicon crystal orientations creating areas of faster or slower oxide growth around the circumference of the silicon cylinder or sphere. Both the diffusivity and the solubility of the oxidant is increased as a result of the tension in the old oxide, while the viscosity of the oxide is decreased.^[2, 3]

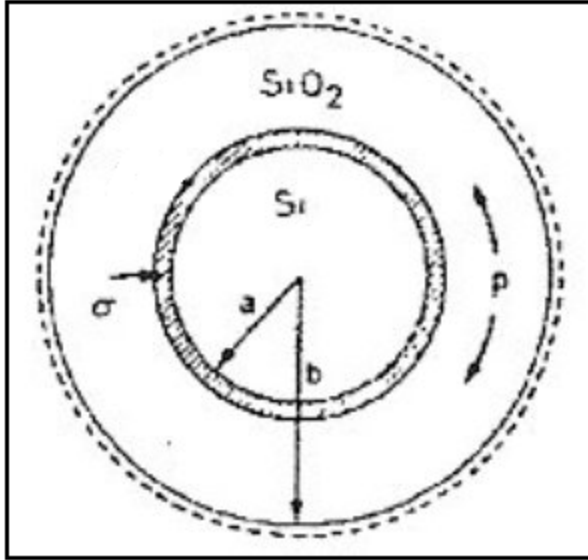


Figure 3.1: Viscous stresses during oxide growth on convex Si structures; P = hydrostatic pressure in the oxide layer creating the tensile stress^[2]

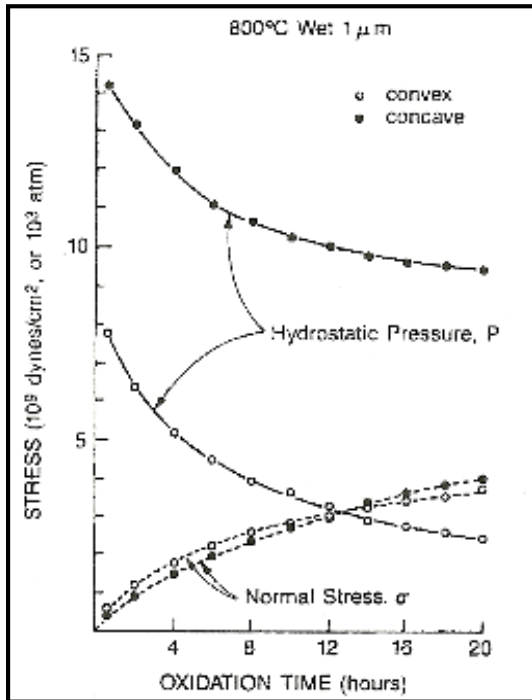


Figure 3.2: Evolution of stress components as a function of oxidation time for both convex and concave silicon geometries^[2]

The normal stress (Figure 3.1) at the Si/SiO₂ interface for a silicon cylinder is given by^[2]:

$$\sigma = -2\eta\beta\left(\frac{1}{a^2} - \frac{1}{b^2}\right) \quad (3.1)$$

and the normal stress (Figure 3.1) at the Si/SiO₂ interface for a silicon sphere is given by ^[5]:

$$\sigma = -4\eta\beta\left(\frac{1}{a^3} - \frac{1}{b^3}\right) \quad (3.2)$$

σ = normal stress at the Si/SiO₂ interface; sign convention is positive for tension and negative for compression

η = viscosity of the oxide

β = velocity constant due viscous flow of bulk oxide

a = radius of silicon core (Figure 2.9 and Figure 3.1)

b = radius of silicon core + oxide layer (Figure 2.9 and Figure 3.1)

The normal stress is compressive and thus it reduces the surface reaction rate (k_s) by adding to the activation energy the extra work which has to be carried out by the expanding oxide.^[5] The reduced reaction rate is represented by:

$$k_s = k_{s0} e^{\frac{\sigma\Omega}{kT}} \quad (3.3)$$

k_{s0} = the stress-free value of k_s given by equations 2.34 and 2.35 for oxygen and water, respectively

Physically the parameter Ω is related to the increase in volume due to the reaction transition of Si to SiO₂. Kao et al.^[2] proposed Ω to be simply the difference of the molecular volume of SiO₂ (45 Å) and the atomic volume of Si (20 Å):

$$\Omega_{SiO_2} - \Omega_{Si} = 25 \text{ \AA} \quad (3.4)$$

Sutardja et al.^[21] and Sutardja and Oldman^[22] suggest that the oxidation reaction of silicon involves the breaking of one Si-Si bond and the attachment of a bridging oxygen atom between the two Si atoms.^[5] In this case Ω must then be close to 12.5 Å, which is the difference between the volume of Si-O (32.5 Å) and Si (20 Å).^[5] As indicated in equation 3.3, the inclusion of the compressive normal stress as a result of expansion, makes the reaction at the Si surface more difficult by affecting the surface reaction rate. The reaction rate decreases at the Si surface as the normal stress compressively increases.

The velocity constant, β , is determined by the creeping flow and continuity equations. Under creeping flow, it is assume the viscosity of silicon dioxide is extremely high and the velocity is very low.^[2] The creeping flow equation relates the oxide velocity to the pressure in the oxide by the following general relationship:

$$\eta\nabla^2 v = \nabla p \quad (3.5)$$

The following two equations expand the creeping flow equation, taking symmetry into consideration, into cylindrical and spherical coordinates, respectively:

$$\eta \left[\frac{1}{r} \frac{\delta}{\delta r} \left(\frac{\delta(rv)}{\delta r} \right) \right] = \frac{\delta p}{\delta r} \quad (3.6)$$

$$\eta \left[\frac{1}{r^2} \frac{\delta}{\delta r} \left(\frac{\delta(r^2v)}{\delta r} \right) \right] = \frac{\delta p}{\delta r} \quad (3.7)$$

The continuity equation is given by the following general relationship:

$$\frac{\delta \rho}{\delta t} = -\nabla \rho v \quad (3.8)$$

Assuming the oxide is incompressible (i.e. constant oxide density, ρ) and expanding the continuity equation into cylindrical and spherical coordinates, respectively yields the following equations:

$$\frac{1}{r} \frac{\delta(rv)}{\delta r} = 0 \quad (3.9)$$

$$\frac{1}{r^2} \frac{\delta(r^2v)}{\delta r} = 0 \quad (3.10)$$

Both equations 3.9 and 3.10 can be solved for the velocity, v resulting in the following two equations for oxide velocity in cylindrical and spherical coordinates, respectively:

$$v(r) = \frac{\beta}{r} \quad (3.11)$$

$$v(r) = \frac{\beta}{r^2} \quad (3.12)$$

The velocity constant β can now be determined from equations 3.11 and 3.12 using the oxide growth rate at the Si/SiO₂ interface.

The other stress component affecting the oxidation of Si is the tensile stress induced by the non-uniform deformation of the old oxide by the newly formed oxide. The hydrostatic pressure (P) in the oxide volume (Figure 3.1) creating the tensile stress in a silicon cylinder is given by^[2]:

$$P = 2\eta\beta \frac{1}{b^2} \quad (3.13)$$

and the hydrostatic pressure (P) in the oxide volume (Figure 3.1) creating the tensile stress in a silicon sphere is given by^[5]:

$$P = 4\eta\beta \frac{1}{b^3} \quad (3.14)$$

This tensile stress, induced by the hydrostatic pressure in the oxide volume, increases the diffusivity (D) and the solubility (C*) of the oxidant and decreases the viscosity of the oxide (η) [9, 11].

$$D = D_o e^{\frac{PV_a}{kT}} \quad (3.15)$$

$$C^* = C_o^* e^{\frac{PV_s}{kT}} \quad (3.16)$$

$$\eta = \eta_o e^{-\alpha P} \quad (3.17)$$

where D_o , C_o^* , and η_o are the zero pressure diffusivity, solubility, and viscosity, respectively. The viscosity of dry oxides is higher than that of wet oxides by two or three orders of magnitude which accounts for the greater retardation despite slower growth rate.^[2] V_a and V_s are the activation volumes of the diffusivity and solubility, respectively, which are defined by the following relationships:

$$V_a = RT \frac{\delta}{\delta P} \left(\ln \frac{D}{D_o} \right) \quad (3.18)$$

$$V_s = RT \frac{\delta}{\delta P} \left(\ln \frac{C^*}{C_o^*} \right) \quad (3.19)$$

α is an empirical constant. Kao et al.^[2] showed that V_s must be of the same order of magnitude as the molecular volume of H_2O (7.5 \AA^3) for wet oxidation. In a similar manner Coffin et al.^[5] considered V_s to be of the order of magnitude of the molecular volume of oxygen (20 \AA^3) for dry oxidation. A large range of values ($75 - 600 \text{ \AA}^3$) can be found in literature for V_a , which were deduced by experimental data fitting. However Kao et al.^[2] and Coffin et al.^[5] suggest, through simulations using V_a in the above stated range, that V_a has no significant impact on the oxidation rate. As a result, Kao et al.^[2] indicate that the variation of the diffusivity with pressure could be described by a temperature dependent activation volume, but adding such complexity would not contribute any new physical insight.

The tensile stress induced by the hydrostatic pressure in the oxide volume increases the diffusivity and solubility as given by equations 3.15 and 3.16, respectively while the viscosity decreases as indicated by equation 3.17. Then, the oxidant transport and the viscous flow properties are enhanced compared to zero pressure conditions^[5]. The two stresses, σ and P , are functions of viscosity as indicated by equations 3.1, 3.2, 3.13 and 3.14, respectively. Viscosity

has strong temperature dependence; consequently both stresses are higher at low temperatures where the viscosity is much larger. The oxide flow becomes more difficult, causing a reduction in the surface reaction rate and both the diffusivity and solubility to increase relative to the planar Si oxidation parameters given by the standard Deal-Grove^[1] model.

CHAPTER 4 - Comparison of Models and Experimental Data

The two modified Deal-Grove^[1] models for the oxidation of cylindrical and spherical silicon structures presented in Chapter 2 predict higher oxidation rates relative to planar silicon structures. Kao et al.^[2] developed a model for the wet oxidation of convex cylindrical silicon structures incorporating the modified Deal-Grove^[1] model for cylinders as presented in Chapter 2 along with the stress effects as presented in Chapter 3. Coffin et al.^[5] developed a model for the dry oxidation of convex spherical silicon structures incorporating the modified Deal-Grove^[1] model for spheres as presented in Chapter 2 along with the stress effects as presented in Chapter 3 in a manner similar to Kao et al.^[2]. The incorporation of stress into both models predict oxide thickness for both cylindrical and spherical structures that differ relative to planar oxides predicted by the standard Deal-Grove^[1] model.

In planar oxidation, as described by the Deal-Grove^[1] model, it is often assumed that the oxide cannot flow and thus undergoes high stress at temperatures lower than 965°C, and that the oxide flows at temperatures higher than 965°C to relieve the stress. This assumption cannot be extended to the oxidation of curved surface such as cylinders and spheres. According to Kao et al.^[2] the substantial oxide growth at 800°C and the retardation at up to 1100°C suggests a continuous temperature dependence of the oxide viscosity. Large stresses may occur in the oxide at higher temperatures and the oxide must be able to flow at low temperatures to justify the extent of oxide deformation on small cylinders.^[2] The stress effects, due to the viscous flow of the oxide must be included to develop a model that is able to accurately predict the oxidation rate of silicon cylinders and spheres.

In the model proposed by Kao et al.^[2] for the oxidation of convex cylindrical silicon the physical parameters in the Deal-Grove^[1] model are modified by the stress caused by the viscous flow of the oxide. The stress normal to the Si/SiO₂ interface decreases the surface reaction rate; the tensile stress in the bulk oxide enhances the oxidant diffusivity and solubility. With the modified physical parameters the model presented by Kao et al.^[2] predicts a thicker oxide than the oxide forming on a flat surface for short oxidation times, and a thinner oxide for long oxidation times (Figure 4.1). The thicker oxide at short oxidation times is due to the tension in the oxide enhancing the oxidant solubility and diffusivity. As oxidation proceeds and the oxide becomes thinner relative to that of a flat surface, the normal stress becomes more

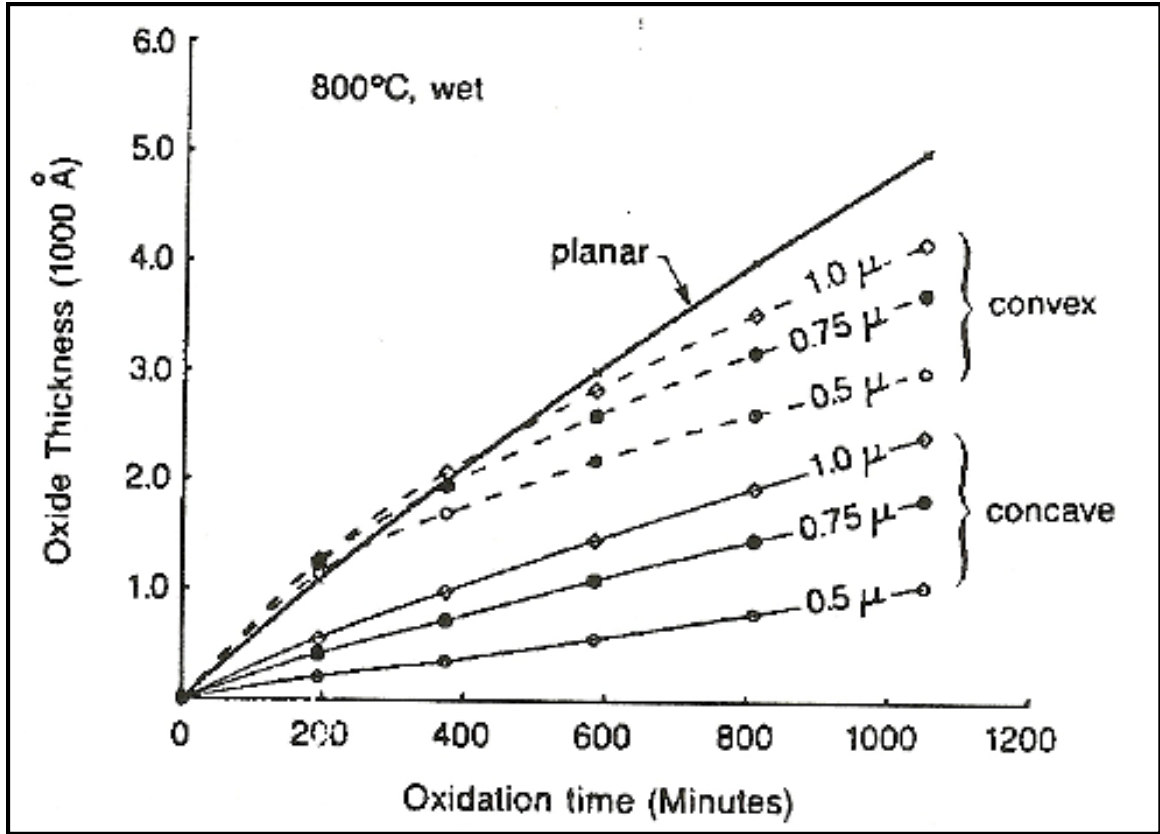


Figure 4.1: Oxide growth of convex and concave cylindrical silicon including stress effects^[2]

important. As the normal stress increases with longer oxidation time oxidation retardation is observed. This in contrast to the stress free model presented in chapter 2, where the oxide is predicted to be thicker than that of a flat surface at longer oxidation times.

Coffin et al.^[5] extended the Deal-Grove^[1] model to spherical coordinates, to describe the oxidation of silicon spheres (i.e. silicon nano-crystals). In their model, Coffin et al.^[5] take into account the effects of stress on the oxidation process in a similar manner to Kao et al.^[2]. They found the physical parameters for the oxidation of spherical silicon are also affected by stress due to the viscous flow of the oxide. The reaction rate constant is retarded by the normal stress at the Si/SiO₂ interface, while the tensile stress in the bulk oxide modifies the oxide viscosity and oxidant solubility. The reaction rate is strongly limited by these stress effects (Figure 4.2). This again is in contrast to the stress free model presented in chapter 2 for spherical silicon oxidation, where the oxide is predicted to be thicker than that of a flat surface at long oxidation times.

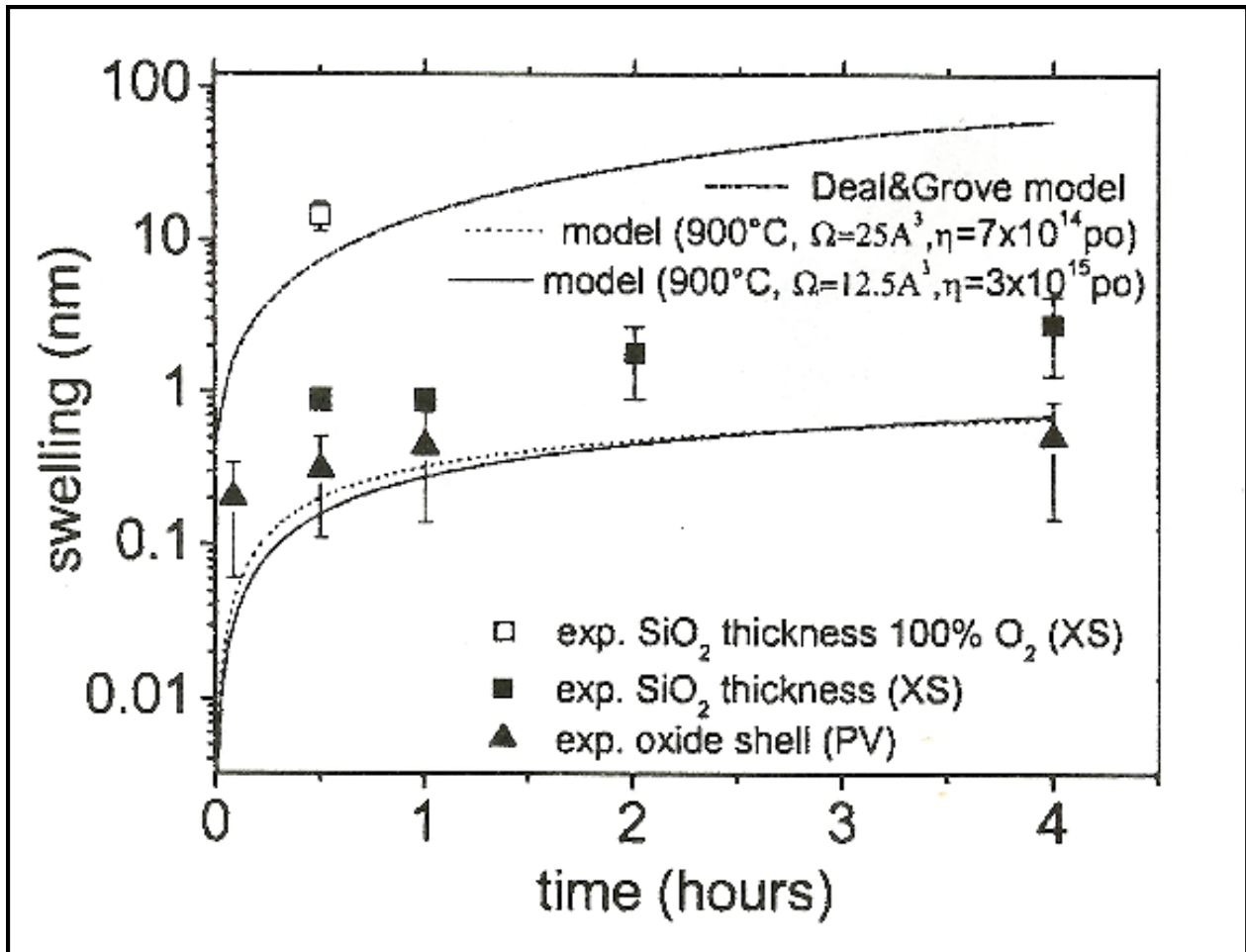


Figure 4.2: Oxide growth of spherical silicon including stress effects^[5]

The effects due to normal compressive stress become even more important as the diameter of the structure decreases in size and the oxide layer becomes thicker (Figure 4.3 – Note: Silicon nano-wires were oxidized for 4 hours at 700°C and 2 hours and 900°C with and without TCA (trichlorethane); The data of interest is without TCA). The normal compressive stress as discussed increasingly slows the rate of the interfacial reaction compared to that of planar silicon. Thus, for Si nano-wires or nano-crystals in the low nano-meter range the retardation of the oxidation, induced by a thick thermally grow oxide layer, is more dramatic than larger diameter structures.

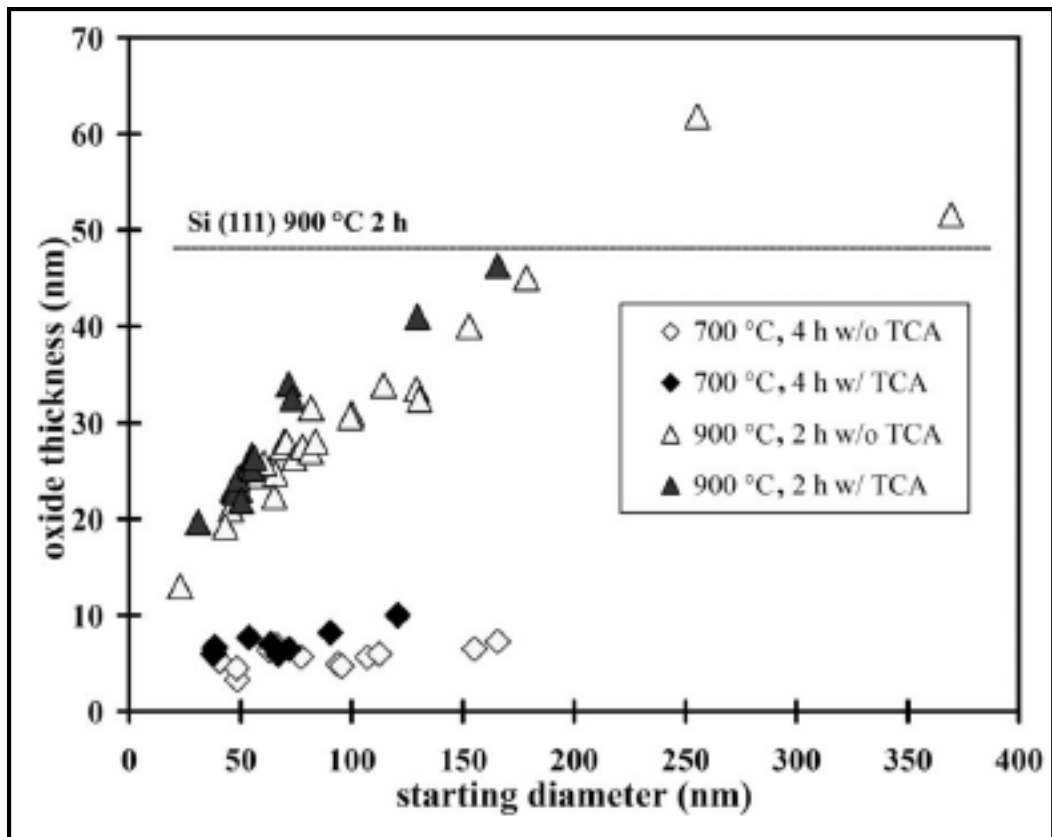


Figure 4.3: Oxide thickness as function of starting diameter for silicon nano-wires^[23]

CHAPTER 5 - Conclusion

With recent progress in the application of silicon nano-wires and nano-crystals in electronic devices, a comprehensive model to describe and predict the oxidation process of non-planar silicon geometries is desirable. The development of nano-electronic devices makes the thermal oxidation of silicon nano-wires (cylinders) and nano-crystals (spheres) important due to the ability to tune the dimensions of these devices through oxidation and subsequent etching. Due to the overall simplicity and popularity of the Deal-Grove^[1] model for the oxidation of flat silicon surfaces it is desirable to adapt this model to other silicon geometries such as cylinders and spheres.

A straightforward extension of the planar Deal-Grove^[1] model to cylindrical and spherical coordinates as described in chapter 2 results in equations that describe the time evolution of the oxidation process for cylindrical and spherical silicon structures, respectively. The modified Deal-Grove^[1] equations (equations 2.58 and 2.94) utilize the same assumptions exploited for the Deal-Grove^[1] model for the oxidation of flat silicon surfaces. However, even with the added complexity due to the change in the geometric structure of the silicon structure being oxidized, equations 2.58 and 2.94 are insufficient to predict accurately the oxidation rates of cylindrical and spherical silicon structures, respectively.

Simply extending the Deal-Grove^[1] model to both cylindrical and spherical coordinates to describe the oxidation of silicon nano-wires and nano-crystals, respectively presents additional complexities that have to be taken into account. First, in contrast to a flat silicon surface, in the oxidation of silicon cylinders and spheres, the change in the surface area of the available silicon for oxidation has to be taken into account. Secondly, the stress induced by the viscous flow of the oxide in non-planar geometries, such as cylinders and spheres, must be taken into account due to its pronounced effect on the physical parameters (i.e. reaction rate constant, diffusivity, viscosity, and solubility).

With the oxidation of planar surfaces, the surface area does not change during oxidation. In contrast, during the oxidation of silicon cylinders and spheres, the core silicon radius decreases as the oxidation process proceeds. This reduction in the core radius decreases the surface area available for oxidation. In cylindrical and spherical silicon oxidation, the core Si radius and the core Si radius + oxide shell radius are not independent variables. The oxide layer

in both geometries is an incompressible fluid and that the ratio of the volume of produced SiO_2 to the volume of consumed Si is 2.25:1. Utilizing these assumptions along with the equations for the volume of a cylinder and a sphere, relationships describing the evolution of the core silicon radius with time are developed (equations 2.71 and 2.104). These time dependent equations describing the evolution of the core silicon radius for both cylindrical and spherical structures, equations 2.71 and 2.104, respectively, are coupled with the modified Deal-Grove^[1] equations in cylindrical and spherical coordinates (equations 2.58 and 2.94) to more accurately describe the oxidation process of these structures.

Another factor that must be accounted for when developing robust models to describe the oxidation of cylindrical and spherical silicon, is the stress induced by the viscous flow of the oxide. In the oxidation of both silicon cylinders and spheres there are two types of stresses that affect the oxidation process. The first is the normal stress at the Si/SiO₂ interface. This normal stress is induced by expansion. Since the volume of SiO₂ is larger than the initial volume of Si consequently the material expands during oxidation thus inducing a normal stress at the interface. This normal stress is compressive and as a result reduces the surface reaction rate (k_s) by adding to the activation energy the extra work which has to be carried out by the expanding oxide. The second stress is the tensile stress induced by the non-uniform deformation of the bulk oxide layer by the newly formed oxide. This tensile stress, induced by the hydrostatic pressure in the oxide volume, increases the diffusivity (D) and the solubility (C^*) of the oxidant and decreases the viscosity of the oxide (η). The importance of these two stress effects is the ultimate retardation of the oxidation process for both silicon cylinders and spheres with respect to planar oxidation. The effects due to these stresses become even more important as the diameter of the structure increasingly decreases in size and the oxide layer becomes thicker.

In conclusion, simply trying to utilize the planar Deal-Grove^[1] model to predict the oxidation of either cylindrical or spherical silicon structures yields exaggerated oxide thicknesses. These exaggerated oxide thicknesses are due to the planar Deal-Grove^[1] model not taking into account the change in available surface area for oxidation and the stress induced due to the viscous flow of the oxide. Both of these factors retard the oxidation rate of non-planar surfaces relative to the oxidation of flat silicon surfaces. This is especially true for small diameter convex silicon structures (i.e. cylinders and spheres) with relatively thick oxide layers. The rate of oxidation is increasingly retarded, relative to planar silicon oxidation, as the diameter

of the structure decreases and the oxide layer thickness increases. Thus, in order to accurately predict oxide thicknesses for non-planar silicon geometries the planar Deal-Grove^[1] model should not be utilized. Instead modified models such as those proposed by Kao et al.^[2] and Coffin et al.^[5] should be employed due to their inclusion of the change of surface area with time and stress effects.

References

- [1] B.E. Deal, A.S. Grove, General Relationship for the Thermal Oxidation of Silicon, *Journal of Applied Physics*, Vol. 36, 12 (1965), 3770 – 3778
- [2] D. B. Kao et al., Two-Dimensional Thermal Oxidation of Silicon-II. Modeling Stress Effects in Wet Oxides, *IEEE Transactions On Electron Devices*, Vol. 35, 1 (1988), 25 – 37
- [3] H. I. Liu, D. K. Biegelsen, et al., Self-Limiting Oxidation for Fabricating Sub-5 nm Silicon Nanowires, *Applied Physics Letters*, Vol. 64, 11 (1994) 1383 - 1385
- [4] R. Okada, S. Iijima, Oxidation Property of Silicon Small Particles, *Applied Physics Letters*, Vol. 58, 15 (1991), 1662 – 1663
- [5] H. Coffin, et al., Oxidation of Si Nanocrystals Fabricated by Ultralow-Energy Ion Implantation in Thin SiO₂ Layers, *Journal of Applied Physics*, Vol. 99, 4 (2006)
- [6] Y.C. Liao, A. M. Nienow, J. T. Roberts, Surface Chemistry of Aerosolized Nanoparticles: Thermal Oxidation of Silicon, *Journal of Physical Chemistry*, Vol. 110, 12 (2006) 6190 – 6197
- [7] Y. Chen, et al., Modeling Silicon Dots Fabrication Using Self-Limiting Oxidation, *Microelectronic Engineering*, Vol. 57 – 58 (2001) 897 – 901
- [8] S. A. Campbell, *Fabrication Engineering at the Micro- and Nanoscale*, New York: Oxford University Press, 2008
- [9] Y. Tu, Amorphous Materials and Interfaces, www.research.ibm.com/amorphous/
- [10] N. Cheung, Thermal Oxidation of Silicon, University of California-Berkley, <<http://www.eng.tau.ac.il/~yosish/courses/vlsi1/I-4-1-Oxidation.pdf>>
- [11] E. A. Lewis, E. A. Irene, The Effect of Surface Orientation on Silicon Oxidation Kinetics, *Journal of the Electrochemical Society*, Vol. 134, 9 (1987), 2332 - 2339
- [12] S. L. Cheng, C. H. Chung, H. C. Lee, A Study of the Synthesis, Characterization, and Kinetics of Vertical Silicon Nanowire Arrays on (001)Si Substrates, *Journal of The Electrochemical Society*, Vol. 155, 11 (2008), D711 - D714
- [13] Y. Cui, Z. Zhong, et al., High Performance Silicon Nanowire Field Effect Transistor, *Nano Letters*, Vol. 3, 2 (2003), 149 - 152
- [14] J. R. Ligenza, W. G. Spitzer, The Mechanisms For Silicon Oxidation in Steam and Oxygen, *Journal of Physics and Chemistry of Solids*, Vol. 14 (1960) 131 – 136

- [15] P. J. Jorgensen, Effect of an Electric Field on Silicon Oxidation, *The Journal of Chemical Physics*, Vol. 37, 4 (1962) 874 – 877
- [16] W. A. Pliskin, R. P. Gnall, Evidence for Oxidation Growth at the Oxide-Silicon Interface From Controlled Etch Studies, *Journal of the Electrochemical Society*, Vol. 111, 7 (1964) 872 – 873
- [17] P. S. Flint, The Rates of Oxidation of Silicon, Paper presented at the Spring Meeting of The Electrochemical Society, Abstract No. 94, Los Angeles, 6 – 10 May 1962
- [18] A. J. Moulson, J. P. Roberts, Water in Silica Glass, *Transactions of the Faraday Society*, Vol. 57, 8 (1961) 1208 – 1216
- [19] F. J. Norton, Permeation of Gaseous Oxygen through Vitreous Silica, *Nature*, Vol. 151, 478 (1961) 701
- [20] C. Single, F. Zhou, H. Hedemeyer, F. E. Prins, D. P. Kern, E. Plies, Oxidation Properties of Silicon Dots on Silicon Oxide Investigated Using Energy Filtering Transmission Electron Microscopy, *Journal of Vacuum Science Technology, B* 16 (6) (1998) 3938 – 3941
- [21] P. Sutardja, W. Oldman, D. B. Kao, Modeling of Stress-Effects in Silicon Oxidation Including the Non-Linear Viscosity of Oxide, *International Electron Devices Meeting*, Vol. 33, (1987) 264 - 267
- [22] P. Sutardja, W. Oldman, Modeling of Stress Effects in Silicon Oxidation, Vol. 36 (1989) 2415 – 2421
- [23] B. Liu, Y. Wang, T. Ho, K. Lew, S.M. Eichfeld, J.M. Redwing, T.S. Mayer, S.E. Mohny, Oxidation of Silicon Nanowires for Top-Gated Field Effect Transistors, *American Vacuum Society*, Vol. 26, 3 (2008) 370 - 374